보건학석사 학위논문

Identification and Characteristics of Long-Range Transport of $PM_{2.5}$ Measured in Three Cities (Beijing, Seoul and Nagasaki)

베이징, 서울, 나가사키에서 측정한 $PM_{2.5}$의
장거리 이동 및 특성 파악

2016년 2월

서울대학교 보건대학원
환경보건학과 대기환경전공
정 승 표

Abstract

Identification and Characteristics of Long-Range Transport of $PM_{2.5}$ Measured in Three Cities (Beijing, Seoul and Nagasaki)

Seung-Pyo Jeong
Department of Environmental Health
Graduate School of Public Health
Seoul National University

$PM_{2.5}$ was sampled in Beijing from November 2014 through April 2015, in Seoul from September 2013 through May 2015, and in Nagasaki from February 2014 to May 2015 during the GRL (Global Research Lab) monitoring campaigns. Chemical species of $PM_{2.5}$ including 3 water-soluble ions (NO_3^-, SO_4^{2-}, NH_4^+), Organic Carbon (OC), Elemental Carbon (EC), and other 17 elements were analyzed. High Concentration Events (HCEs) of $PM_{2.5}$ were classified according to the National Ambient Air Quality Standards (NAAQS) of 24-h $PM_{2.5}$ standard in three countries (China, South Korea and Japan) over the monitoring campaigns.

From the Residence Time Analysis (RTA) results, the HCEs of $PM_{2.5}$ in Beijing were observed for 52 days (out of total 111 sampling days) and 14 days were determined as Long-Range Transport (LRT) events. In Seoul, HCEs were observed for 92 days (out of total 279 sampling days) and LRT events occurred for 64 days. In Nagasaki, only 15 days (out of total 245 days) were determined as the HCEs and LRT events occurred for 13 days.

$PM_{2.5}$ average concentrations of Beijing, Seoul, and Nagasaki were found to be 118, 44, and 18 $\mu g/m^3$ over the study period. In terms of characteristics of $PM_{2.5}$ chemical species during each classified events, for LRT event, $PM_{2.5}$ mass levels were found to be 151, 79, and 48 $\mu g/m^3$ in Beijing, Seoul, and Nagasaki, whereas for the Local event, $PM_{2.5}$ levels were 238, 65, 48 $\mu g/m^3$ in Beijing, Seoul, and Nagasaki.

Cluster analysis showed that sulfate was significantly increased when air parcels moved towards the coastline of China and the Yellow Sea. In case of LRT event and Local event in three cities (Beijing, Seoul and Nagasaki), the PSCF results showed the different potential sources regions contributing to the elevated $PM_{2.5}$ concentrations at each sampling site.

Keywords: $PM_{2.5}$, High Concentration Events (HCEs), Long-Range Transport (LRT) event, Local event, Residence Time Analysis (RTA), Cluster analysis, Potential Source Contribution Function (PSCF)

Student Number: 2014-23362

Contents

List of Tables

List of Figures

1. Introduction

Ambient particulate matter ($PM_{2.5}$) is known to affect directly and indirectly on human health expressed as increased mortality and morbidity (Brunekreef and Holgate, 2002; III and Dockery, 2006) and increased light scattering and less visibility (Hwang and Hopke, 2007).

Differentiating the contribution of Long-Range Transport (LRT) and local atmospheric, in affecting $PM_{2.5}$ levels, is important for determining effective measure (Healy et al., 2012). This is particularly true in China, which is one of the most polluted country in Asia (Chan and Yao, 2008). Beijing, the capital of China, is encountering serious air pollution problems including extremely high concentrations of $PM_{2.5}$ in the atmosphere (Zheng et al., 2005). Seoul, the capital of South Korea, is affected by air pollution, such as $PM_{2.5}$, from the Asian Continent (Kang et al., 2004). Nagasaki is located around the continent of Asia and also seems to be affected by the air parcel from the East Asian continent. In fact, the "Kosa" phenomena, a kind of haze due to LRT of soil dusts originating from the Chinese desert such as Gobi Desert, has been occasionally observed in Nagasaki (Uematsu et al., 1983).

Over the last several decades, trajectory analysis has been used to assess transport patterns of air parcels (Stohl, 1998; Luo and Rossow, 2004). Backward trajectory has been used for the visualization of movement of air parcels and their possible contributions to pollutant levels have been evaluated by statistical methods (Karaca and Camci, 2010). Residence Time Analysis (RTA) represents the amount of time that an air parcels have spent in different grid cells before arriving at the

receptor site and can cause the effect that a source in each grid cell would have at the sampling sites (Poirot et al., 2001; Salvador et al., 2008). A number of researches have been using cluster analysis, which is the categorization of backward trajectories to figure comparable characteristics of transportation (He et al., 2003; Jorba et al., 2004; Abdalmogith and Harrison, 2005; Borge et al., 2007). Potential Source Contribution Function (PSCF), used in several studies (Lee et al., 2003; Kim et al., 2007; Heo et al., 2009), is the generation of conditional probability grids around a receptor site for selected high level events of a pollutant (over the criterion value) (Ashbaugh et al., 1985).

This study offers a method for evaluating the contribution of LRT and local patterns of $PM_{2.5}$, in urban (Beijing and Seoul) and background site (Nagasaki). The proposed approach includes 3 main stages: (i) High Concentration Events (HCEs) of $PM_{2.5}$ were classified according to the National Ambient Air Quality Standards (NAAQS) of 24-h $PM_{2.5}$ standard in three countries (China, South Korea and Japan); (ii) HCEs were classified as LRT event and Local event by RTA; (iii) Cluster analysis and PSCF were used to verify the characteristics of LRT event and Local event.

2. Materials and methods

2.1. Sampling and analysis

$PM_{2.5}$ samples were collected every third day over a 24-h period from 2013 to 2015 (in Beijing from November 2014 to April 2015; in Seoul from September 2013 to May 2015; in Nagasaki from February 2014 to May 2015). The sampling sites (Fig. 1) were located on the roof of the school of public health building at Peking University (N: 39.983, E: 116.355), Seoul National University (N: 37.581, E: 127.001) and Nagasaki University (N: 32.772, E: 129.868).

$PM_{2.5}$ were sampled on a Teflon filter (47 mm Pall, 1 μm pore size), quartz fiber filter (47 mm Whatman) and Zefluor filter (47 mm Pall, 1 μm pore size) with a low volume air sampler consisting of a cyclone (2.5 μm size cut, URG-2000-30EH), vacuum pumps and dry gas meters. Teflon filters and quartz fiber filters were collected at 16.7 L/min for trace elements and carbon species, respectively. Zefluor filters were collected at 10.0 L/min flow rate for ionic species. Precision of the flow data was ± 5 %.

Fig. 1. Geographical location of the sampling site.

$PM_{2.5}$ mass were measured by analytical balance (reading precision 10 μg) on Teflon filters stabilizing for ~24-h at constant temperature (20.0 ± 2 °C) and relative humidity (45 ± 5 %). Also, Teflon filters used to analysis trace elements using X-Ray Fluorescence (XRF) by Clarkson University in New York. Zefluor filters were extracted for 3-h in 30 mL ultrapure water (resistivity ≈ 18.2 MΩ cm) in an ultrasonic bath. After filtration through microporous PTFE membranes (PALL Acrodisc CR, pore size 0.45 μm), three ions (NH_4^+, NO_3^-, SO_4^{2-}) were determined by ion chromatography (IC, Dionex DX-120). Quartz fiber filters were pre-baked at 450 °C during 12- h for lower their carbon blanks, and analyzed using the standard Thermal/Optical Transmission (TOT) analysis method (NIOSH method 5040) described in detail by Birch and Cary (1996).

2.2. QA/QC

For quality assurance of the samples, Teflon filters and lab blank were weighed thrice. If the difference in weight between the thrice times were less than or equal to 3 μg, that weighing was considered as suitable. If the differences were more than 3 μg, the procedure was repeated. Filter blanks were prepared in the same way as the samples. Lab blanks were used to investigate possible contaminants from handling samples in the laboratory. Analyzing both filter blanks and lab blanks, concentrations from filter blanks were subtracted from the sample, while the lab blanks were used to see whether any interference exists. At least 10 % of the samples were analyzed by spiking with a known amount of ion species and carbon to calculate the recovery efficiencies. The results of recovery efficiency tests indicated the ranges of recovery efficiency among every 10 samples varied from 95 to 105 %. The reproducibility test varied between 90 and 110 % for all the chemical species.

3. Model descriptions

3.1. Residence Time Analysis (RTA)

In this study, the Hybrid Single-Particle Lagrangian Integrated Trajectory 4 (HYSPLIT4) (Draxler and Rolph, 2003) was used to compute backward trajectories endpoints. To assess the accuracy of a trajectory, different balloons were used, and the average accuracy after 48 h was over 80% (Stohl, 1998). Considering mixing height of a ground-based sampling site may have led to more accurate trajectory calculations since it was important figure whether contaminants coming out from the source mixes in planetary boundary layer (PBL) (Junquera et al., 2005). Also the selection of appropriate air parcel arrival height representing the mixing height was critical to identifying the source areas and LRT using the hybrid receptor model (Jeong et al., 2011). Thus, five day backward trajectories for every hour planetary boundary layer (PBL) mixing heights were calculated during the total sampling period using the Global Data Assimilation System (GDAS) 0.5° meteorological data.

Eight countries were classified for RTA by the borderline of each country (Russia, Kazakhstan, Mongolia, China, North Korea, South Korea, Japan and Taiwan) and the minimum unit of grid was 0.5° (Fig. 2). Each backward trajectory endpoint indicated hourly residence in the grid classified by each country. Thus, the total 'residence time' of each country was the whole time that air parcel spent in the total grid of each country (Hopke, 2003). The residence time values related to levels of concentration could be allocated to analyze likely directions from which contaminated air was transported to the sampling site.

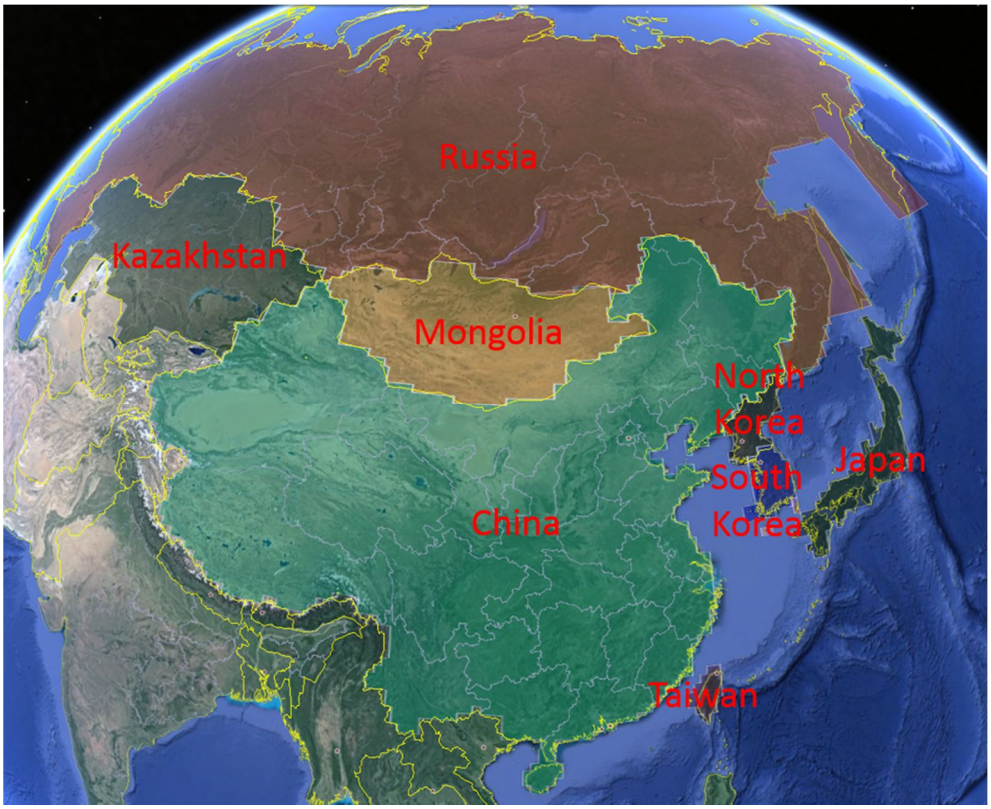

Fig. 2. Eight countries (Russia, Kazakhstan, Mongolia, China, North Korea, South Korea, Japan and Taiwan) classified for RTA using Google Earth.

3.2. Cluster analysis

A number of trajectories arriving at a sampling sites over the study period can be analyzed to identify similar atmospheric transport patterns. Applying cluster analysis, also known as a multivariate statistical technique has been performed to investigate the structure of geographical data (Stohl, 1998). Several studies have used cluster analysis to indicate individual backward trajectories to a relatively small number of different groups (Borge et al., 2007; Kong et al., 2010).

3.3. Potential Source Contribution Function (PSCF)

The PSCF values for each of the single grid cell are calculated by counting the number of trajectory segment endpoints (Hsu et al., 2003). The number of endpoints included in the *ij*-th cell is denoted as n_{ij}. m_{ij} is defined as the number of endpoints of which pollutant concentrations exceed a criterion value for the same cell. The PSCF value for the *ij*-th cell is then denoted as

$$\mathrm{PSCF}_{ij} = \frac{\mathrm{m}_{ij}}{\mathrm{n}_{ij}} \times W_{ij}$$

High PSCF values indicates the arrival of air parcels at a receptor site with pollutant concentrations higher than a criterion value. These cells indicate potential sources that contributions to the pollution at a receptor site. In this study, the criterion values are determined by high concentrations which are over the NAAQS of 24-h $PM_{2.5}$ standard in three countries. W_{ij} is an empirical weight function suggested by Zeng and Hopke (1989) to reduce the overestimate of small n_{ij} on the PSCF values:

$$W_{ij} = \begin{cases} 1.0 & \mathrm{n}_{ij} > 2 \cdot Avg \\ 0.75 & Avg < \mathrm{n}_{ij} \le 2 \cdot Avg \\ 0.5 & 0.5 \cdot Avg < \mathrm{n}_{ij} \le Avg \\ 0.25 & 0 < \mathrm{n}_{ij} \le 0.5 \cdot Avg \end{cases}$$

where *Avg* is the average number of trajectory segment endpoints in all cells (Xu and Akhtar, 2010).

4. Results and discussion

4.1. Residence Time Analysis (RTA)

Table 1 showed the result of RTA in Beijing. HCEs of $PM_{2.5}$ were 52 days, out of total 111 sampling days, over the NAAQS of China (24-h standard, 75 $\mu g/m^3$). For HCEs of Beijing, the average residence time (RT) of China was the highest (46 %), followed by Russia (21 %) and Mongolia (19 %). LRT event in Beijing was classified when the residence times of Russia, Mongolia or Kazakhstan were higher than China; LRT events were 14 days and Local events were 38 days. LRT events in Beijing, the average RT of Russia was 44 % and that of Mongolia was 24 %, higher than China and air parcels stayed around Russia and Mongolia for a long time relatively. Local events in Beijing, the average RT of China was 56 % and significantly higher than the other countries.

Table 2 showed the result of RTA in Seoul. HCEs of $PM_{2.5}$ were 92 days, out of total 279 sampling days, over the NAAQS of South Korea (24-h standard, 50 $\mu g/m^3$). For HCEs of Seoul, the average RT of China was the highest (32 %), followed by South Korea (17 %), Russia (10 %) and North Korea (9 %). The average RT of China was much higher than South Korea, so this should be considered to classify LRT event of Seoul. Thus LRT event of Seoul was defined when the difference between RT of South Korea and China was higher than that of HCEs in Seoul (15 %), or RT of Russia, Mongolia or Kazakhstan exceeded RT of South Korea; LRT events were 64 days and Local events were 28 days. For LRT events, the average RT of China was 38 % and that of Mongolia was 13 %, and air parcels stayed longer than South Korea. Local events in Seoul, the average RT of

South Korea was 29 % and that of China was 18 %.

Table 3 showed the result of RTA in Nagasaki. HCEs of $PM_{2.5}$ were only 15 days, out of total 245 sampling days, over the NAAQS of Japan (24-h standard, 35 $\mu g/m^3$). For HCEs of Nagasaki, the average RT of China was the highest (31 %), followed by Japan (12 %) and Mongolia (9 %). The average RT of China was much higher than Japan, and this tendency was also shown in the results of Seoul. Therefore, LRT event of Nagasaki was defined when the difference between RT of Japan and China was higher than that of HCEs in Nagasaki (19 %), or RT of Mongolia, South Korea, Russia or North Korea exceeded RT of Japan; LRT events were 13 days and Local events were 2 days. For LRT events, the average RT of China was 33 %, while that of Japan was 10 %. The average RT of Japan was 29 %, followed by China was 17% in Local events. In case of Local events in Seoul and Nagasaki, the differences with the average RT of China were not significantly different. This indicated that a considerable air parcels from China arrived at Seoul and Nagasaki, in spite of their Local events.

Table 1. Results of RTA in Beijing.

China		Russia		Mongolia		Kazakhstan	
Mean ± SD	RT CV	Mean ± SD	RT CV	Mean ± SD	RT CV	Mean ± SD	RT CV
Total (n=111)							
High concentration events (n=52)							
1342 ± 671	46 50	617 ± 546	21 89	559 ± 335	19 60	245 ± 237	8 97
Long-range transport events (n=14)							
541 ± 155	19 29	1274 ± 445	44 35	697 ± 361	24 52	298 ± 255	10 86
Local events (n=38)							
1637 ± 530	56 32	374 ± 343	13 92	508 ± 315	17 62	226 ± 231	8 102

SD-Standard Deviation.

RT-Residence Time, %.

CV-Coefficient of Variation, %.

Table 2. Results of RTA in Seoul.

South Korea			China			Russia			North Korea			Mongolia			Kazakhstan		
Mean ± SD	RT	CV	Mean ± SD	RT	CV	Mean ± SD	RT	CV	Mean ± SD	RT	CV	Mean ± SD	RT	CV	Mean ± SD	RT	CV
Total (n=279)																	
High concentration events (n=92)																	
492 ± 341	17	69	926 ± 473	32	51	287 ± 420	10	146	247 ± 228	9	92	171 ± 208	6	121	28 ± 102	1	369
Long-range transport events (n=64)																	
334 ± 184	12	55	1103 ± 407	38	37	365 ± 463	13	127	255 ± 232	9	91	214 ± 230	7	107	34 ± 120	1	358
Local events (n=28)																	
852 ± 344	29	40	522 ± 352	18	67	107 ± 215	4	201	228 ± 221	8	97	73 ± 93	3	127	14 ± 33	1	237

SD-Standard Deviation.

RT-Residence Time, %.

CV-Coefficient of Variation, %.

Table 3. Results of RTA in Nagasaki.

Japan			China			Mongolia			South Korea			Russia			North Korea		
Mean ± SD	RT	CV	Mean ± SD	RT	CV	Mean ± SD	RT	CV	Mean ± SD	RT	CV	Mean ± SD	RT	CV	Mean ± SD	RT	CV
Total (n=245)																	
High concentration events (n=15)																	
359 ± 248	12	69	895 ± 344	31	38	240 ± 257	8	107	217 ± 274	7	126	113 ± 235	4	207	35 ± 45	1	128
Long-range transport events (n=13)																	
282 ± 143	10	51	958 ± 319	33	33	259 ± 268	9	103	222 ± 294	8	133	130 ± 249	4	191	40 ± 47	1	117
Local events (n=2)																	
857 ± 217	29	25	487 ± 214	17	44	119 ± 168	4	141	185 ± 74	6	40	3 ± 4	0	141	5 ± 6	0	141

SD-Standard Deviation.

RT-Residence Time, %.

CV-Coefficient of Variation, %

Table 4 showed that statistical analysis of chemical species of LRT events and Local events of $PM_{2.5}$ in three cities (Beijing, Seoul and Nagasaki). The $PM_{2.5}$ average concentrations of Beijing, Seoul and Nagasaki were found to be 118, 44 and 18 $\mu g/m^3$ in total, 151, 79 and 48 $\mu g/m^3$ in LRT event and 238, 65, 48 $\mu g/m^3$ in Local event, respectively. The average $PM_{2.5}$ concentrations of Beijing and Seoul seriously exceeded $PM_{2.5}$ concentrations of the NAAQS. The $PM_{2.5}$ mass concentration of Local events was higher than that of LRT events in Beijing, while the $PM_{2.5}$ mass concentration of Local events was lower than that of LRT events in Seoul. Also, high sulfate concentrations were found in LRT events of Beijing and Local events of Seoul. It has been suggested that high $PM_{2.5}$ and sulfate concentrations were affected by combustion of fossil fuels and rapid industrialization in China.

Figure 3 showed the frequencies of occurrence of both LRT event and Local event in three cities. $PM_{2.5}$ average mass concentration was weighted to frequencies for identification of the effects of HCEs. It has been reported that increased $PM_{2.5}$ mass concentration and adverse health effect have the significant positive correlation (Dockery and Pope, 1994; Brunekreef and Holgate, 2002). In Beijing, the frequency of Local event was higher than that of LRT event and the effect was more significant when $PM_{2.5}$ average mass concentration was weighted. On the other hand, frequency of LRT event was higher than that of Local event in Seoul. When $PM_{2.5}$ average mass concentration was weighted, the frequency of LRT event greatly increased to 41 % and this clearly indicated that Seoul was highly affected by LRT of $PM_{2.5}$. Although HCEs in Nagasaki was only around 6 % because it was rural background site, HCEs increased to around 16 % when $PM_{2.5}$

average mass concentration was weighted. This indicated that Nagasaki was also highly affected by LRT.

The NO_3^-/SO_4^{2-} mass ratio indicated the relative importance of mobile vs. stationary sources of sulfur and nitrogen in the atmosphere (Yao et al., 2002; Y. Wang et al., 2006). The high ratio of NO_3^-/SO_4^{2-} was related to the majority of mobile source over stationary source of pollutants (Arimoto et al., 1996). The estimated mass ratios of NO_X to SO_X from the emissions of gasoline and diesel fuel burning were 13:1 and 8:1, respectively (Shen et al., 2008). In China, the sulfur content in coal was 1 % and the estimated mass ratio of NO_X to SO_X was 1:2 from coal burning (Li et al., 2008). Figure 4 showed NO_3^-/SO_4^{2-} mass ratios related to LRT and Local event. The NO_3^-/SO_4^{2-} mass ratios of Beijing were high, compared to Seoul and Nagasaki. It was because of high NO_3^- concentration derived from the emission of vehicle exhaust (diesel and gasoline) in Beijing. The mass ratio of NO_3^-/SO_4^{2-} was relatively low when Local event occurred compared to LRT event, because the increase of SO_4^{2-} was relatively greater than the NO_3^-. It had been suggested that Local event in Beijing, the effect of stationary sources was greater than automobile combustion. The mass ratio of NO_3^-/SO_4^{2-} in Seoul was lower when LRT event occurred than Local event. This indicated that the main source of Local event was gasoline and diesel combustion from automobiles and the main source of LRT event was stationary sources. The mass ratio of NO_3^-/SO_4^{2-} in Nagasaki was lower when HCEs occurred, owing to large increase of SO_4^{2-}. The increase of SO_4^{2-} related to secondary sulfate as well as stationary emission. Higher SO_4^{2-} values in HCEs may be attributable to secondary chemical reaction which formed from LRT and stagnation of air parcels from stationary source.

Elemental Carbon (EC) was a byproduct of incomplete combustion of Organic Carbon (OC) (Chu, 2005). EC has been used as a marker of primary OC in evaluation of the secondary organic carbon concentrations since it is emitted mainly from primary combustion sources (Cao et al., 2004). The quantification and separation of primary and secondary organic carbon have been known to be significantly important in controlling particulate carbon pollution as well as in exploring secondary aerosol formation (Turpin et al., 2000; Fuzzi et al., 2006; Hallquist et al., 2009). The OC/EC mass ratio in source emissions compared to that ratio in atmospheric samples can be the indicator of the presence of Secondary Organic Aerosol (SOA) formation (Zhang et al., 2005; Docherty et al., 2008). The high OC/EC ratios might be associated with the formation of secondary aerosols (Na et al., 2004; X. Wang et al., 2006).

The observed values of OC/EC in this study were 10.5, 11.7 and 12.6, for total sampling days, LRT event and Local event in Beijing, 7.9, 8.0 and 8.5 in Seoul, 8.4, 6.2 and 4.9 in Nagasaki (Fig. 5), demonstrating that SOA may be a significant contributor to $PM_{2.5}$. The reason of relatively low ratio of OC/EC in HCEs of Nagasaki is because of the rapid increase of EC concentration compared to OC concentration. This suggests that there is the effect of primary combustion emission from stationary sources nearby sampling sites. The correlation of OC and EC was also used to estimate the origin of OC and EC (Saylor et al., 2006). As shown in Table 5, good OC–EC correlations were obtained with correlation coefficient (R) of 0.946, 0.730 and 0.920 for total samplings, LRT events and Local events in Beijing, respectively. The correlations suggested the existence of common dominant sources for OC and EC (e.g. motor vehicle exhaust, coal combustion). OC and EC were correlated well in $PM_{2.5}$, indicating that the byproducts of combustion process and secondary chemical reaction concentrated in fine particles (Kong et al., 2010). It has been suggested that Local event in Beijing was greatly affected by common dominant sources of local emissions, while LRT event in Seoul was highly affected by long-range transported sources.

Table 4. Statistical analysis of chemical species of LRT events and Local events of $PM_{2.5}$.

Species	Beijing (average ± SD, $\mu g/m^3$)			Seoul (average ± SD, $\mu g/m^3$)			Nagasaki (average ± SD, $\mu g/m^3$)		
	Total	LRT events	Local events	Total	LRT events	Local events	Total	LRT events	Local events
Cr	0.02 ± 0.01	0.02 ± 0.01	0.03 ± 0.02	0.01 ± 0.03	0.01 ± 0.01	0.03 ± 0.08	0.01 ± 0.00	0.01 ± 0.00	0.01 ± 0.00
Ni	0.26 ± 0.12	0.27 ± 0.11	0.32 ± 0.12	0.08 ± 0.02	0.08 ± 0.02	0.09 ± 0.02	0.09 ± 0.02	0.08 ± 0.02	0.08 ± 0.00
Cu	0.16 ± 0.10	0.17 ± 0.07	0.23 ± 0.12	0.06 ± 0.01	0.06 ± 0.01	0.06 ± 0.01	0.05 ± 0.01	0.05 ± 0.00	0.05 ± 0.00
Zn	0.40 ± 0.49	0.52 ± 0.28	0.77 ± 0.66	0.11 ± 0.06	0.16 ± 0.08	0.14 ± 0.04	0.05 ± 0.03	0.11 ± 0.04	0.12 ± 0.05
Br	0.08 ± 0.08	0.10 ± 0.07	0.14 ± 0.10	0.03 ± 0.02	0.04 ± 0.02	0.04 ± 0.02	0.01 ± 0.01	0.02 ± 0.01	0.00 ± 0.00
Pb	0.10 ± 0.12	0.11 ± 0.08	0.19 ± 0.16	0.02 ± 0.02	0.04 ± 0.02	0.02 ± 0.01	0.01 ± 0.01	0.02 ± 0.01	0.02 ± 0.00
S	2.76 ± 3.66	2.28 ± 1.18	5.78 ± 4.94	1.73 ± 1.02	2.46 ± 1.23	2.40 ± 0.81	1.41 ± 0.91	3.07 ± 1.05	3.42 ± 0.04
Al	0.79 ± 0.86	0.87 ± 0.37	1.47 ± 1.05	0.59 ± 1.24	1.16 ± 2.44	0.64 ± 0.53	0.37 ± 0.62	1.85 ± 1.72	2.55 ± 0.60
Si	3.33 ± 2.96	3.09 ± 1.47	4.88 ± 3.36	2.39 ± 5.36	4.85 ± 10.5	2.55 ± 2.28	1.40 ± 2.65	7.76 ± 7.34	10.7 ± 2.62
Ti	0.13 ± 0.13	0.12 ± 0.04	0.21 ± 0.17	0.07 ± 0.12	0.13 ± 0.24	0.08 ± 0.05	0.04 ± 0.05	0.16 ± 0.14	0.21 ± 0.06
Fe	1.15 ± 0.77	1.14 ± 0.39	1.74 ± 0.99	0.49 ± 0.51	0.77 ± 0.98	0.54 ± 0.21	0.31 ± 0.23	0.91 ± 0.62	1.09 ± 0.26
Mg	0.51 ± 0.58	0.47 ± 0.20	0.73 ± 0.86	0.22 ± 0.41	0.40 ± 0.79	0.19 ± 0.20	0.19 ± 0.28	0.90 ± 0.83	1.07 ± 0.23
Na	1.46 ± 1.31	1.89 ± 0.90	2.42 ± 1.63	0.44 ± 0.28	0.65 ± 0.36	0.42 ± 0.15	0.60 ± 0.39	0.87 ± 0.40	0.71 ± 0.11
Cl	4.89 ± 5.60	7.47 ± 4.27	9.03 ± 6.63	0.52 ± 0.63	1.00 ± 0.83	0.67 ± 0.78	0.14 ± 0.23	0.17 ± 0.20	0.09 ± 0.02
Ca	1.21 ± 0.90	1.35 ± 0.67	1.79 ± 1.02	0.39 ± 0.64	0.72 ± 1.23	0.38 ± 0.23	0.21 ± 0.36	1.07 ± 1.07	1.27 ± 0.28
K	1.91 ± 2.32	2.05 ± 0.85	3.65 ± 3.19	0.52 ± 0.46	0.92 ± 0.77	0.65 ± 0.33	0.24 ± 0.25	0.88 ± 0.58	1.08 ± 0.15
Mn	0.07 ± 0.07	0.07 ± 0.03	0.13 ± 0.09	0.03 ± 0.02	0.04 ± 0.04	0.03 ± 0.01	0.02 ± 0.01	0.05 ± 0.02	0.05 ± 0.02
Sr	0.03 ± 0.08	0.02 ± 0.01	0.06 ± 0.13	0.01 ± 0.01	0.01 ± 0.01	0.01 ± 0.01	0.00 ± 0.01	0.01 ± 0.01	0.01 ± 0.00
V	0.01 ± 0.01	0.01 ± 0.00	0.01 ± 0.02	0.01 ± 0.01	0.01 ± 0.01	0.01 ± 0.01	0.01 ± 0.00	0.01 ± 0.01	0.01 ± 0.00
NH_4^+	4.90 ± 5.18	2.55 ± 2.25	7.46 ± 5.28	7.59 ± 5.78	12.1 ± 5.33	11.0 ± 2.85	0.81 ± 0.43	1.07 ± 0.27	1.47 ± 0.19
NO_3^-	7.26 ± 8.84	7.43 ± 4.25	13.6 ± 11.0	5.16 ± 4.88	6.99 ± 6.75	9.81 ± 6.13	1.91 ± 2.36	2.65 ± 3.98	1.02 ± 1.06
SO_4^{2-}	4.18 ± 5.96	3.23 ± 2.31	8.31 ± 6.56	7.00 ± 7.02	11.3 ± 9.47	9.83 ± 3.94	2.95 ± 2.16	4.87 ± 1.90	7.56 ± 0.53
OC	33.5 ± 33.8	48.9 ± 21.2	61.3 ± 40.1	8.15 ± 4.32	11.7 ± 6.05	9.75 ± 3.58	4.10 ± 2.06	6.21 ± 4.39	4.68 ± 0.47
EC	2.88 ± 2.35	4.15 ± 1.37	4.85 ± 2.65	1.47 ± 2.41	2.79 ± 4.56	1.21 ± 0.42	0.50 ± 0.28	1.07 ± 0.77	0.98 ± 0.30
$PM_{2.5}$	118 ± 132	151 ± 79	238 ± 152	44 ± 28	79 ± 33	65 ± 14	18 ± 11	48 ± 10	48 ± 6

SD-Standard Deviation.

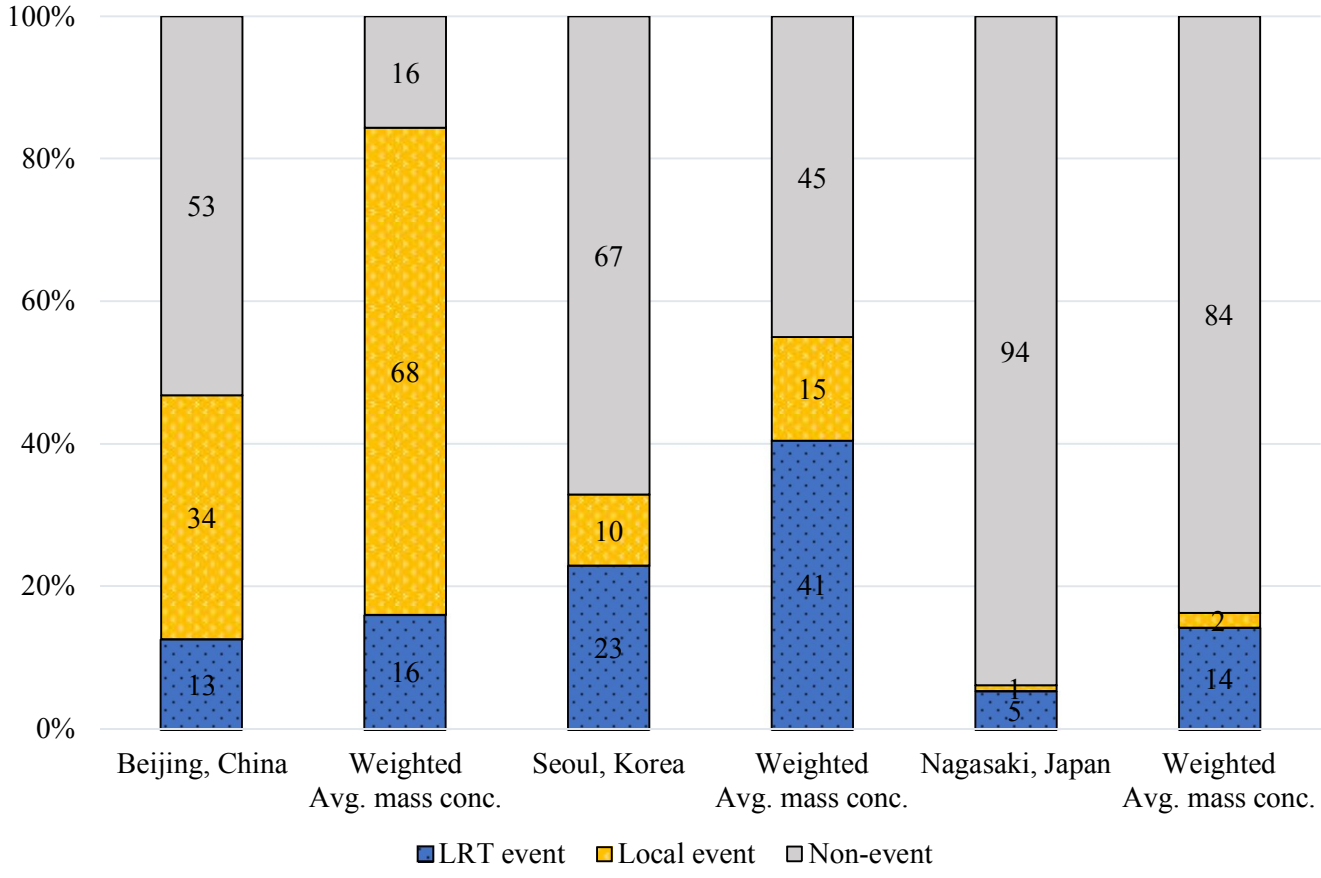

Fig. 3. Frequencies of occurrence of both LRT event and Local event in Beijing, Seoul and Nagasaki.

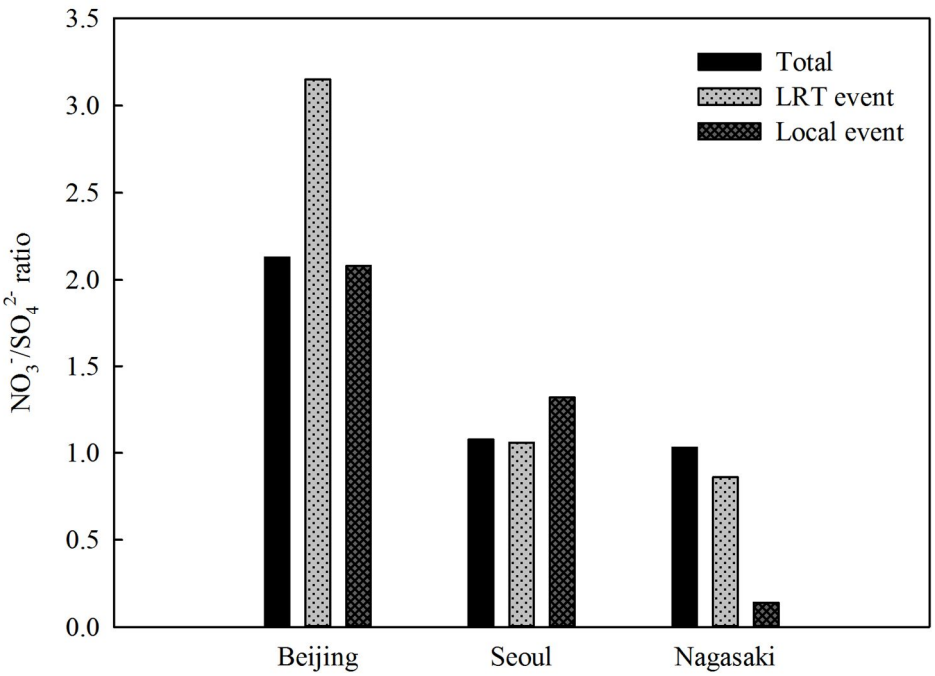

Fig. 4. NO_3^-/SO_4^{2-} ratios for total sampling days, LRT event and Local event in Beijing, Seoul and Nagasaki.

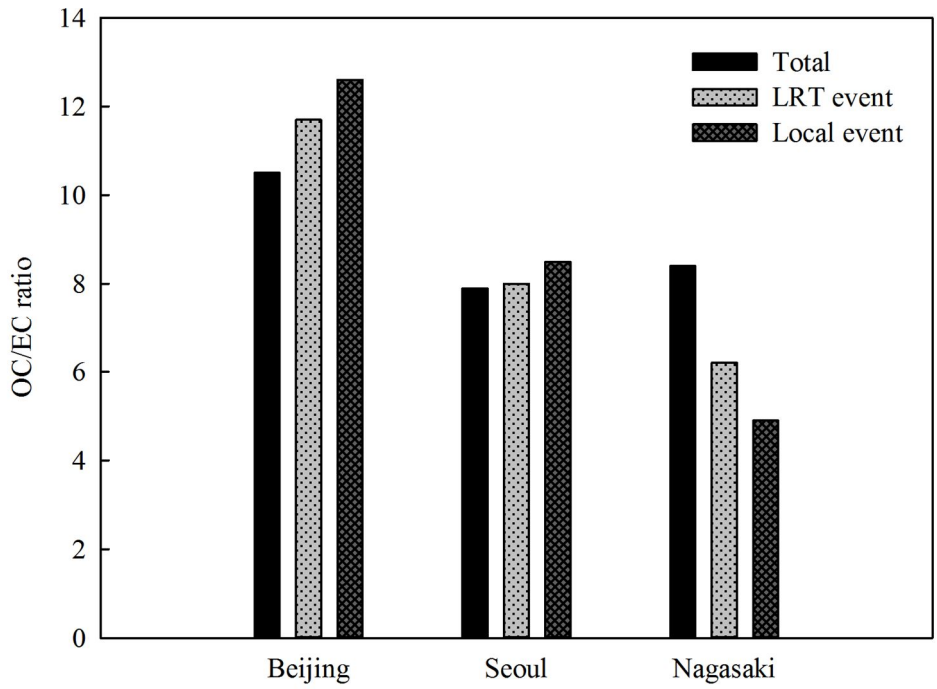

Fig. 5. OC/EC ratios for total sampling days, LRT event and Local event in Beijing, Seoul and Nagasaki.

Table 5. Pearson correlation coefficient (R) between OC and EC concentrations for total sampling days, LRT event and Local event in Beijing, Seoul and Nagasaki.

	R (*p*-value)		
	Total	LRT event	Local event
Beijing	0.946 (<0.001)	0.730 (0.005)	0.920 (<0.001)
Seoul	0.593 (<0.001)	0.647 (<0.001)	0.279 (0.151)
Nagasaki	0.633 (<0.001)	0.949 (<0.001)	-

4.2. Cluster analysis

According to the percent change in Total Spatial Variance (TSV), the number of clusters is subjectively chosen for the result. For much of the clustering it typically increases at a small, constant rate, but at the particular point it increases rapidly, indicating that the clusters being combined are not very similar (Draxler et al., 2009). Generally, pairing "different" clusters is indicated by 30 % change in the variation of TSV. Figure 6 showed the results of the changes in TSV according to the numbers of clusters for LRT event and Local event in Beijing, Seoul and Nagasaki.

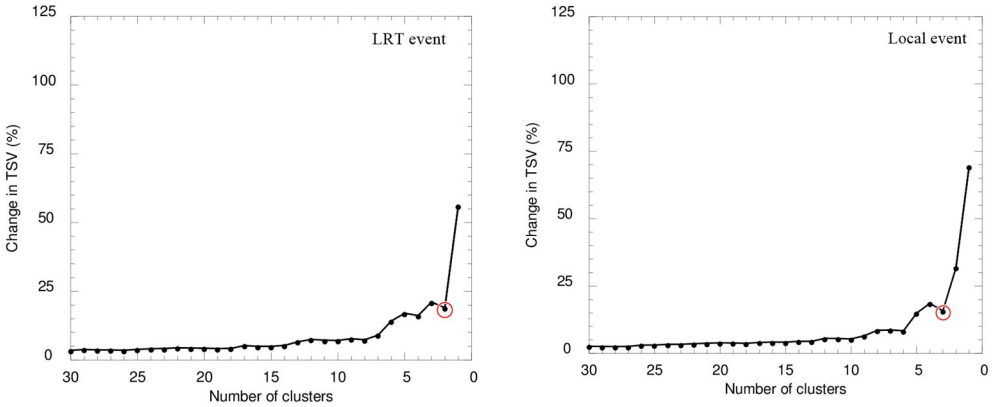

(a) Beijing

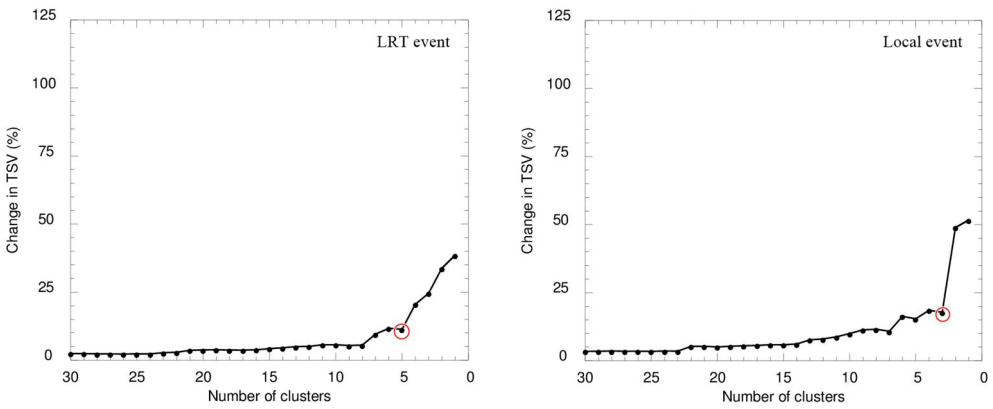

(b) Seoul

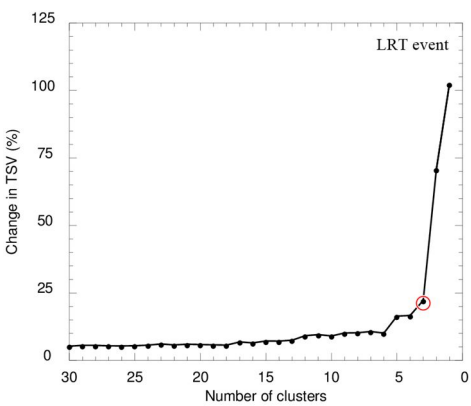

(c) Nagasaki

Fig. 6. Percent change of TSV in three cities. Red circles indicated that the number of clusters selected for LRT event and Local event.

4.2.1. Beijing

In LRT event of Beijing, the trajectories were categorized into 2 sectors for LRT event and 3 sectors for Local event according to the air parcel transport (Fig. 7). In the LRT event of Beijing, two typical air parcels trajectories were from Russia (sector 1 accounting for 42 % from northwest), and the border between north Kazakhstan and Russia (sector 2 accounting for 58 % from northwest), respectively. The triangle symbols were marked every 6 hours and the distances between each of them were almost the same, indicating that air parcels moved in a constant speed. In sector 1 and 2, air parcels arrived at Beijing passed through only 1-day out of 5-day backward trajectory, thus sector 1 and 2 were classified as LRT events. Starting height and trajectory height of sector 1 were constantly higher than those of sector 2. Different air parcels were consist of different chemical species with the aerosols by transporting through different areas, and therefore the distribution of chemical species among different air parcels could shed light on their possible sources (Wang et al., 2005).

The Student's *t*-test and one-way ANOVA (using SPSS software, version 12) were used to identify differences in concentrations, and resulted for cluster analysis of LRT event and Local event, respectively. Table 6 statistically summarized the chemical species of $PM_{2.5}$ in Beijing, according to each sector of LRT events and Local events by cluster analysis. In LRT event, concentrations of potassium, manganese and sulfate of sector 2 were significantly higher than sector 1 ($p < 0.01$). Potassium was one of the most important major emissions from biomass burning (Simoneit, 2002) and manganese could be represented as crustal element (Duvall et al., 2008). It has been suggested that the concentrations of potassium and manganese were high because of the effect of biomass burning while passing through the border between Russia, Kazakhstan and Mongolia and longer time of stagnation in deserts of Mongolia. In Local event, concentrations of titanium, magnesium and strontium of sector 3 were significantly higher than those of the other sectors ($p < 0.05$). Titanium and magnesium were typical crustal elements (Skinner, 1979) and strontium also could be classified as crustal element because there is about 370 ppm of Sr (0.037 %) and it's fifteenth most abundant element (James, 1982). Sector 3 suggested that air parcels were considerably affected by LRT since backward trajectories passed through Russia, Kazakhstan and Mongolia, which are the regions that include abundant crustal elements.

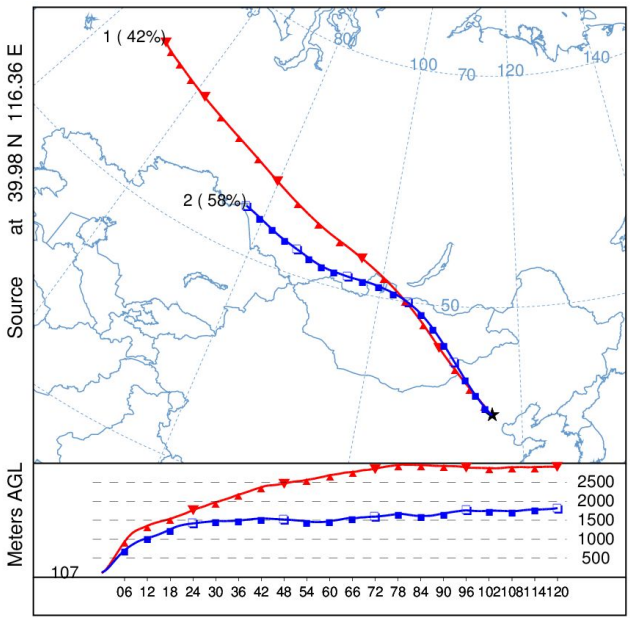

(a) LRT event

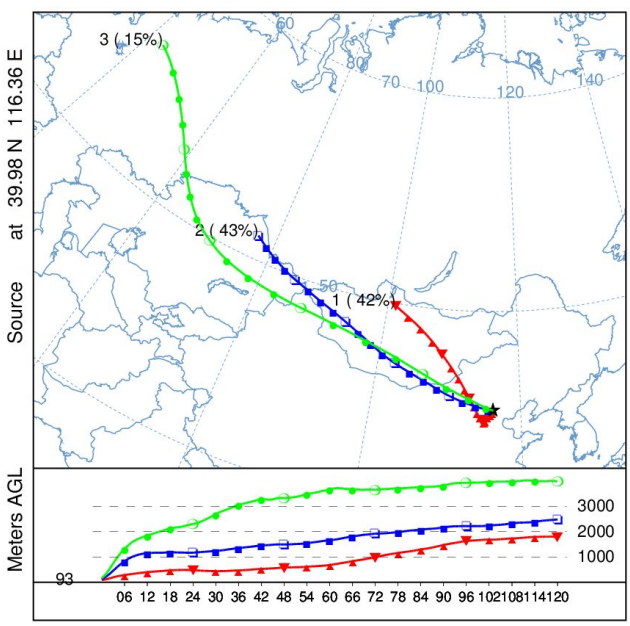

(b) Local event

Fig. 7. Backward trajectory clusters in Beijing.

Table 6. Statistical analysis of chemical species for each group in Beijing by cluster analysis.

Species	LRT event (average ± SD, $\mu g/m^3$)		Local event (average ± SD, $\mu g/m^3$)		
	Sector 1 (42%)	Sector 2 (58%)	Sector 1 (42%)	Sector 2 (43%)	Sector 3 (15%)
Cr	0.02 ± 0.00	0.03 ± 0.01	0.03 ± 0.02	0.04 ± 0.02	0.03 ± 0.01
Ni	0.27 ± 0.11	0.27 ± 0.12	0.30 ± 0.12	0.35 ± 0.14	0.32 ± 0.06
Cu	0.16 ± 0.04	0.18 ± 0.10	0.23 ± 0.13	0.23 ± 0.12	0.23 ± 0.11
Zn	0.37 ± 0.14	0.72 ± 0.31	0.94 ± 0.89	0.72 ± 0.42	0.46 ± 0.34
Br	0.06 ± 0.03	0.15 ± 0.08	0.16 ± 0.13	0.13 ± 0.08	0.09 ± 0.07
Pb	0.07 ± 0.03	0.16 ± 0.10	0.18 ± 0.16	0.17 ± 0.13	0.23 ± 0.21
S	1.45 ± 0.29	3.38 ± 0.98	6.56 ± 5.70	5.84 ± 5.01	3.65 ± 1.53
Al	0.72 ± 0.14	1.07 ± 0.49	1.21 ± 0.83	1.29 ± 0.59	2.55 ± 1.78
Si	2.44 ± 0.74	3.97 ± 1.80	4.64 ± 3.51	4.67 ± 2.31	6.00 ± 5.25
Ti	0.10 ± 0.02	0.15 ± 0.05	0.17 ± 0.11	0.19 ± 0.09	0.39 ± 0.33
Fe	0.99 ± 0.13	1.33 ± 0.54	1.70 ± 1.12	1.81 ± 0.99	1.65 ± 0.70
Mg	0.41 ± 0.07	0.56 ± 0.29	0.52 ± 0.36	0.55 ± 0.27	1.75 ± 1.76
Na	1.45 ± 0.38	2.46 ± 1.11	2.56 ± 1.77	2.54 ± 1.71	1.79 ± 1.09
Cl	5.42 ± 2.71	10.2 ± 4.64	9.80 ± 7.76	9.18 ± 6.25	6.75 ± 4.63
Ca	1.06 ± 0.38	1.73 ± 0.82	1.89 ± 1.26	1.76 ± 0.85	1.63 ± 0.89
K	1.55 ± 0.52	2.73 ± 0.74	3.02 ± 2.08	3.19 ± 1.80	6.37 ± 6.26
Mn	0.05 ± 0.02	0.09 ± 0.03	0.14 ± 0.12	0.12 ± 0.07	0.10 ± 0.05
Sr	0.02 ± 0.00	0.03 ± 0.01	0.03 ± 0.02	0.03 ± 0.02	0.22 ± 0.30
V	0.00 ± 0.00	0.01 ± 0.00	0.01 ± 0.01	0.01 ± 0.01	0.03 ± 0.03
NH_4^+	1.18 ± 0.92	4.21 ± 2.32	7.68 ± 5.46	7.88 ± 5.48	5.30 ± 4.71
NO_3^-	5.75 ± 2.49	9.39 ± 5.24	13.9 ± 9.58	14.0 ± 12.8	12.0 ± 10.7
SO_4^{2-}	2.30 ± 1.47	4.63 ± 2.84	7.50 ± 6.06	9.45 ± 7.32	7.43 ± 6.49
OC	41.5 ± 17.1	57.5 ± 23.8	72.7 ± 46.2	55.5 ± 33.3	50.1 ± 41.9
EC	3.87 ± 1.35	4.48 ± 1.44	5.31 ± 2.72	4.82 ± 2.87	3.87 ± 1.94
$PM_{2.5}$	132 ± 92	177 ± 57	233 ± 133	245 ± 160	231 ± 201

SD-Standard Deviation.

4.2.2. Seoul

In Seoul, the trajectories were categorized into 5 sectors for LRT event and 3 sectors for Local event according to the air parcel transports (Fig. 8). For LRT event, backward trajectory of sector 1 departed from east China passed through the Yellow Sea in a slow speed and then reached Seoul. Backward trajectories of sector 2 and sector 3 departed from central region of Russia and the border between Russia and China passed through North Korea and then reached Seoul. In sector 2 and sector 3, air parcels rapidly reached the border between North Korea and South Korea in 4 days, and air parcels were stagnated around South Korea for one day. Backward trajectories of sector 4 and sector 5 were affected by westerlies and air parcels quickly passed through Mongolia and China. For Local event, sector 1 showed the similar route with LRT event of sector 3. Air parcels of sector 2 did not stagnate in China but instantly passed through the Yellow Sea and reached South Korea. Backward trajectories of sector 3 reached South Korea very rapidly passing through Russia, Kazakhstan, Mongolia, China and North Korea in 4 days. Even though air parcels were transported long-range, the effects were classified as domestic effects by RTA, because RT of the air parcels in South Korea was longer than the other countries. Starting heights of trajectories tended to be high and air parcels tended to transport in high altitudes with the longer distances of backward trajectories.

Table 7 statistically summarized the chemical species of $PM_{2.5}$ in Seoul, according to each sector of LRT event and Local event by cluster analysis. In LRT event, concentrations of sulfur and sulfate of sector 1 were significantly high, compared to the other sectors ($p < 0.01$). Air parcels passed through the sea could bring a large amount of chemical species from marine. Sulfur was emitted from the combustion of fossil fuel in industrial area of East China and emission passed through sea. The production of aerosol sulfate was enhanced in the air that contained a significant amount of seal-salt aerosol due to the higher pH associated with newly formed sea-salt-nucleated cloud droplets when compared to those formed on sulfate aerosol (O'Dowd et al., 1999). Likewise, sector 2 of Local event, concentrations of sulfur and sulfate, which had a typical route passing the Yellow sea, were significantly higher than those of sector 1 ($p < 0.05$).

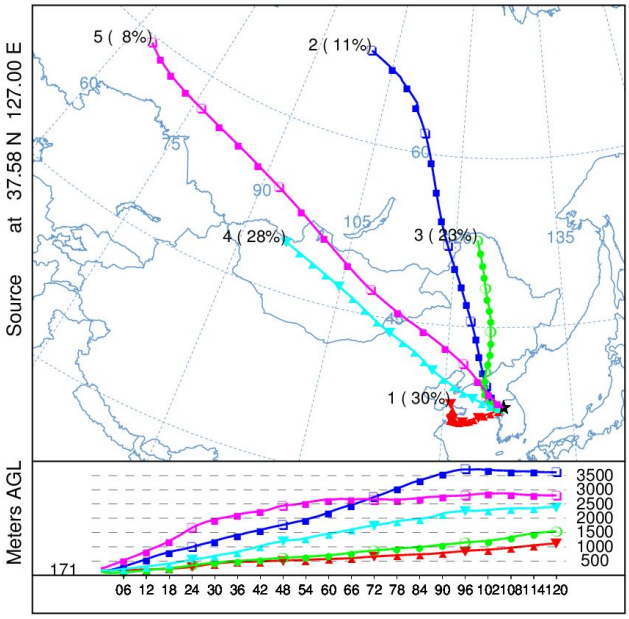

(a) LRT event

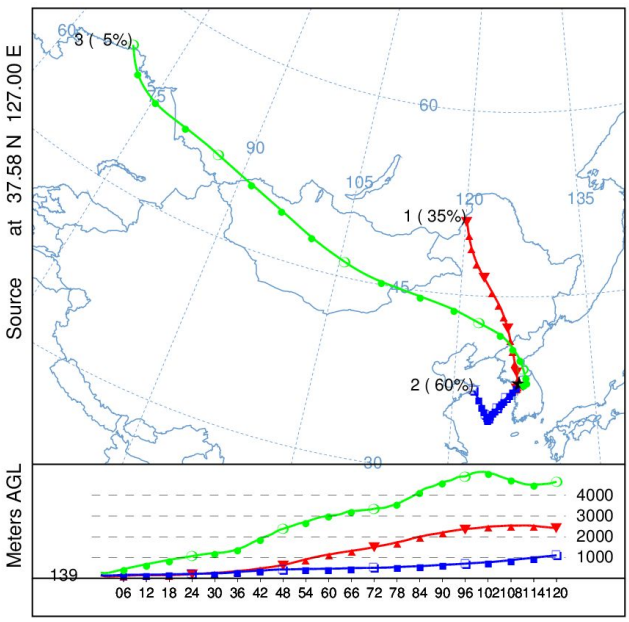

(b) Local event

Fig. 8. Backward trajectory clusters in Seoul.

Table 7. Statistical analysis of chemical species for each group in Seoul by cluster analysis.

Species	LRT event (average ± SD, $\mu g/m^3$)					Local event (average ± SD, $\mu g/m^3$)		
	Sector 1 (30%)	Sector 2 (11%)	Sector 3 (23%)	Sector 4 (28%)	Sector 5 (8%)	Sector 1 (35%)	Sector 2 (60%)	Sector 3 (5%)
Cr	0.01 ± 0.00	0.01 ± 0.00	0.01 ± 0.01	0.01 ± 0.00	0.01 ± 0.00	0.01 ± 0.00	0.04 ± 0.11	0.01
Ni	0.08 ± 0.01	0.08 ± 0.01	0.08 ± 0.02	0.08 ± 0.02	0.07 ± 0.00	0.09 ± 0.01	0.08 ± 0.02	0.08
Cu	0.06 ± 0.01	0.06 ± 0.01	0.06 ± 0.01	0.07 ± 0.01	0.05 ± 0.00	0.06 ± 0.01	0.06 ± 0.01	0.05
Zn	0.20 ± 0.07	0.10 ± 0.03	0.16 ± 0.11	0.17 ± 0.06	0.13 ± 0.04	0.14 ± 0.05	0.14 ± 0.04	0.10
Br	0.04 ± 0.03	0.04 ± 0.02	0.04 ± 0.02	0.05 ± 0.02	0.03 ± 0.01	0.04 ± 0.02	0.03 ± 0.02	0.04
Pb	0.04 ± 0.03	0.02 ± 0.01	0.03 ± 0.02	0.04 ± 0.02	0.02 ± 0.01	0.02 ± 0.01	0.02 ± 0.01	0.02
S	3.51 ± 1.09	1.17 ± 0.54	2.09 ± 0.94	2.33 ± 1.04	1.82 ± 1.01	1.82 ± 0.75	2.75 ± 0.67	2.25
Al	0.97 ± 1.15	0.55 ± 0.38	1.80 ± 4.57	1.19 ± 1.66	0.70 ± 0.62	0.46 ± 0.18	0.75 ± 0.65	0.48
Si	3.98 ± 4.80	2.27 ± 1.82	7.68 ± 19.8	4.94 ± 7.04	2.92 ± 2.80	1.78 ± 0.65	3.05 ± 2.81	1.96
Ti	0.10 ± 0.09	0.07 ± 0.03	0.20 ± 0.45	0.14 ± 0.18	0.08 ± 0.05	0.07 ± 0.02	0.09 ± 0.07	0.05
Fe	0.68 ± 0.39	0.50 ± 0.11	1.00 ± 1.81	0.84 ± 0.75	0.51 ± 0.18	0.48 ± 0.10	0.58 ± 0.25	0.40
Mg	0.38 ± 0.59	0.18 ± 0.14	0.56 ± 1.39	0.41 ± 0.54	0.22 ± 0.18	0.14 ± 0.08	0.22 ± 0.24	0.14
Na	0.64 ± 0.42	0.49 ± 0.14	0.67 ± 0.41	0.77 ± 0.34	0.47 ± 0.09	0.43 ± 0.15	0.41 ± 0.16	0.38
Cl	0.66 ± 0.70	0.93 ± 0.97	1.23 ± 0.95	1.22 ± 0.77	0.84 ± 0.72	1.19 ± 1.08	0.40 ± 0.34	0.20
Ca	0.63 ± 0.77	0.46 ± 0.27	0.95 ± 2.05	0.83 ± 1.17	0.35 ± 0.15	0.35 ± 0.15	0.41 ± 0.27	0.27
K	0.85 ± 0.60	0.58 ± 0.17	1.11 ± 1.29	1.03 ± 0.52	0.62 ± 0.18	0.66 ± 0.30	0.65 ± 0.36	0.51
Mn	0.05 ± 0.02	0.03 ± 0.01	0.05 ± 0.07	0.05 ± 0.03	0.03 ± 0.01	0.03 ± 0.01	0.03 ± 0.01	0.02
Sr	0.01 ± 0.01	0.01 ± 0.00	0.01 ± 0.02	0.01 ± 0.01	0.01 ± 0.00	0.01 ± 0.01	0.01 ± 0.00	0.00
V	0.02 ± 0.01	0.01 ± 0.01	0.01 ± 0.01	0.01 ± 0.01	0.01 ± 0.01	0.01 ± 0.01	0.02 ± 0.01	0.01
NH_4^+	12.4 ± 6.75	8.01 ± 4.52	13.2 ± 4.12	11.2 ± 4.66	11.4 ± 1.30	7.97 ± 0.14	12.6 ± 2.47	9.57
NO_3^-	7.17 ± 9.80	7.89 ± 6.74	6.75 ± 5.00	7.48 ± 5.61	4.35 ± 2.51	11.1 ± 6.44	9.43 ± 5.87	1.94
SO_4^{2-}	18.6 ± 11.2	3.49 ± 2.11	7.55 ± 5.58	11.0 ± 8.51	7.85 ± 4.95	7.23 ± 3.21	11.5 ± 3.65	9.57
OC	11.9 ± 9.24	10.3 ± 4.79	12.4 ± 4.60	12.5 ± 3.58	8.14 ± 2.38	11.8 ± 4.56	8.38 ± 2.18	12.8
EC	3.89 ± 6.26	1.29 ± 0.84	1.35 ± 0.72	3.64 ± 5.40	1.91 ± 1.54	1.29 ± 0.57	1.15 ± 0.33	1.27
$PM_{2.5}$	85 ± 34	69 ± 13	83 ± 46	81 ± 26	59 ± 2	69 ± 19	63 ± 11	60

SD-Standard Deviation.

4.2.3. Nagasaki

Clusters of Nagasaki were affected by westerlies and were classified by the lengths of backward trajectories (Fig. 9). Backward trajectory of sector 1 departed from west Mongolia, passed through east China and the Yellow sea, then reached Nagasaki. Sector 2, backward trajectory departed from east China and stagnated in China for one to two days. In Sector 3, the starting area was west Russia and air parcels rapidly arrived at Nagasaki.

Table 8 statistically summarized the chemical species of $PM_{2.5}$ in Nagasaki, according to each sector of LRT event and Local event by cluster analysis. For sector 1 of LRT event, concentration of crustal elements (sum of Si, Ti, Fe, Mg, Na) was significantly higher than sector 2 ($p < 0.01$). It was suggested that sector 1 was significantly affected by crustal elements, and the air parcels passed through desert of China and Mongolia.

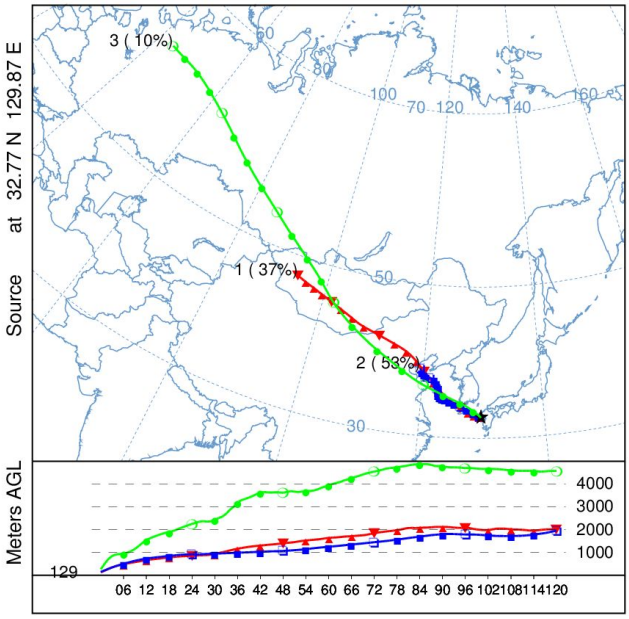

LRT event

Fig. 9. Backward trajectory clusters in Nagasaki.

Table 8. Statistical analysis of chemical species for each group in Nagasaki by cluster analysis.

Species	LRT event (average ± SD, μg/m^3)		
	Sector 1 (37%)	Sector 2 (53%)	Sector 3 (10%)
Cr	0.02 ± 0.00	0.01 ± 0.00	0.01
Ni	0.07 ± 0.00	0.08 ± 0.02	0.11
Cu	0.05 ± 0.00	0.05 ± 0.00	0.05
Zn	0.14 ± 0.05	0.09 ± 0.02	0.03
Br	0.01 ± 0.01	0.02 ± 0.01	0.01
Pb	0.02 ± 0.01	0.02 ± 0.00	0.01
S	2.98 ± 0.72	3.48 ± 0.86	0.72
Al	3.05 ± 1.76	0.67 ± 0.39	4.12
Si	12.8 ± 7.41	2.70 ± 1.66	17.9
Ti	0.26 ± 0.14	0.06 ± 0.03	0.36
Fe	1.34 ± 0.63	0.48 ± 0.14	1.77
Mg	1.47 ± 0.94	0.32 ± 0.16	1.43
Na	1.08 ± 0.41	0.68 ± 0.33	1.19
Cl	0.11 ± 0.03	0.14 ± 0.10	0.78
Ca	1.84 ± 1.32	0.41 ± 0.23	1.81
K	1.36 ± 0.58	0.47 ± 0.18	1.36
Mn	0.07 ± 0.02	0.03 ± 0.00	0.07
Sr	0.02 ± 0.02	0.01 ± 0.00	0.02
V	0.02 ± 0.01	0.01 ± 0.01	0.01
NH_4^+	1.00 ± 0.25	1.14 ± 0.30	3.45
NO_3^-	1.21 ± 0.19	3.61 ± 5.37	3.12
SO_4^{2-}	5.40 ± 1.14	5.07 ± 1.82	0.80
OC	5.03 ± 0.54	7.37 ± 5.90	3.99
EC	1.03 ± 0.27	1.17 ± 1.04	0.56
$PM_{2.5}$	50.0 ± 14.2	45.8 ± 7.16	57.5

SD-Standard Deviation.

4.3. Potential Source Contribution Function (PSCF)

4.3.1. Beijing

The results of the PSCF analysis for LRT event and Local event in Beijing were represented in Figure 10. In LRT event, it could be seen that high PSCF values for $PM_{2.5}$ was found along east Kazakhstan (Fig. 10(a)). Kazakhstan has an abundant supply of accessible mineral and fossil fuel resources. East Kazakhstan along with Balkhsah has been known to be the place abundant of mineral resources and the resources have been actively mined.

For Local event, the areas near Bohai Bay in southeast Beijing were identified as potential sources (Fig. 10(b)). Tianjin and Tangshan nearby Bohai Bay were located in the central section of the circum-Bohai Sea Gulf region. Tangshan is the largest heavy-industry city with a long history in the Beijing–Tianjin–Hebei regions. Pollution from coal emissions has increased dramatically since the 1990s following the rapid growth of Tangshan's industrial sector (Li et al., 2013).

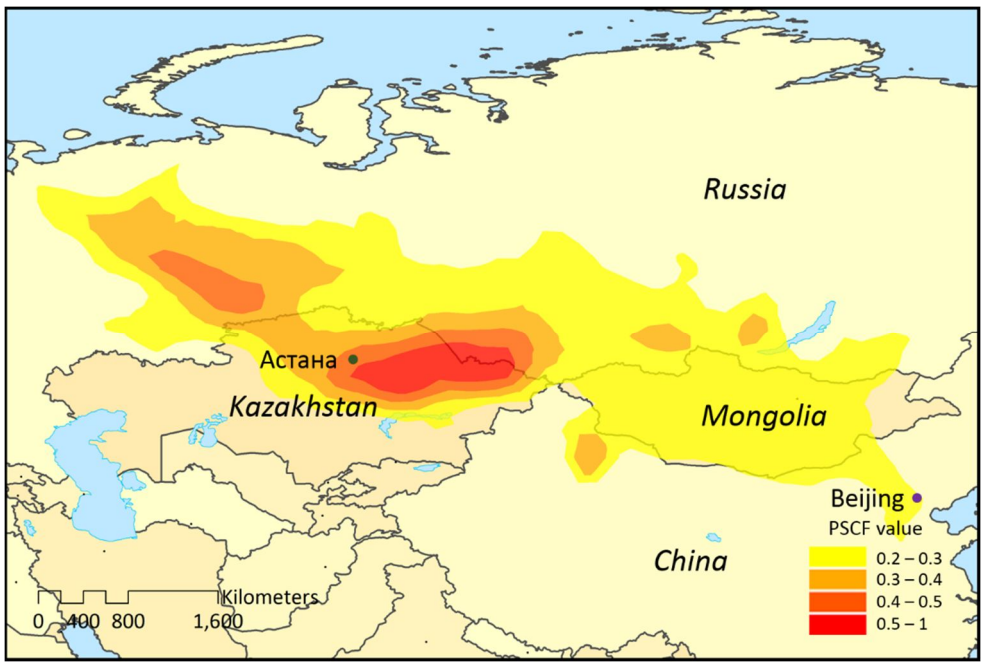

(a) LRT event

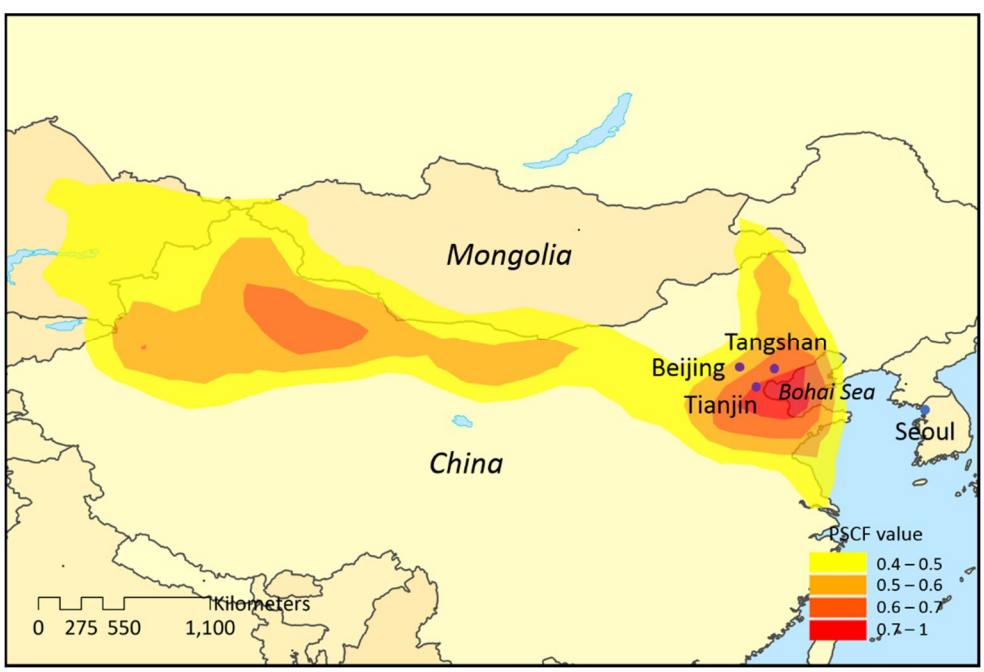

(b) Local event

Fig. 10. PSCF plots for $PM_{2.5}$ in Beijing.

4.3.2. Seoul

For LRT event of Seoul, it could be seen that high PSCF values for $PM_{2.5}$ was found along Shandong Province (Fig. 11(a)). Shandong Province, located on the northeast coast of China and adjacent to South Korea and Japan across the Bohai Sea, contributes the largest amount of SO_2, NO_X and PM emissions in China (Geng et al., 2009). High emissions of air pollutants arise mainly from coal combustion, coupled with the complex terrain and anti-cyclone system below an altitude of 600 m in Shandong Province, which results in a serious impact on urban and rural air quality. Jinan, the capital of Shandong Province, had a population of about 3.53 million in 2010, and is located less than 500 km south of Beijing. In the World Bank list of twenty most polluted cities exposed to the highest concentrations of PM in 2004, Jinan ranked twelfth (The World Bank). Furthermore, fine PM dominated the components of PM_{10} in Jinan with a large ratio of $PM_{2.5}/PM_{10}$ (between 0.24 and 0.92), which was generally attributed to secondary aerosol formation of species such as sulfate and nitrate (Cheng et al., 2011). Therefore, the special geographical situation and serious air pollution of Jinan made it a important location in East Asia.

For Local event (Fig. 11(b)), the high PSCF values was found nearby Seoul, especially Taean an Ansan. Major point sources such as thermoelectric power plants and petrochemical complexes are located in Taean. And there are about 1800 small factories emitting pollutants into the atmosphere in the small 6 km×4 km Sihwa industrial complex area in Ansan (Park et al., 2001). The complex is consisted of metallurgical industry, chemical manufacturing, coating industry, paper printing, and waste incineration facilities etc. Solvent use in organic chemical and metallurgical processes, and waste incineration result in emission of many organic compounds, including VOCs and PAHs, to the atmosphere (Park et al., 2001). Seoul is the capital city of South Korea with about 10.1 million people in 605.21 km^2 area. Heavy transportation is major local source of air pollution in Seoul. In 2015, about 3.0 million vehicles were registered in Seoul.

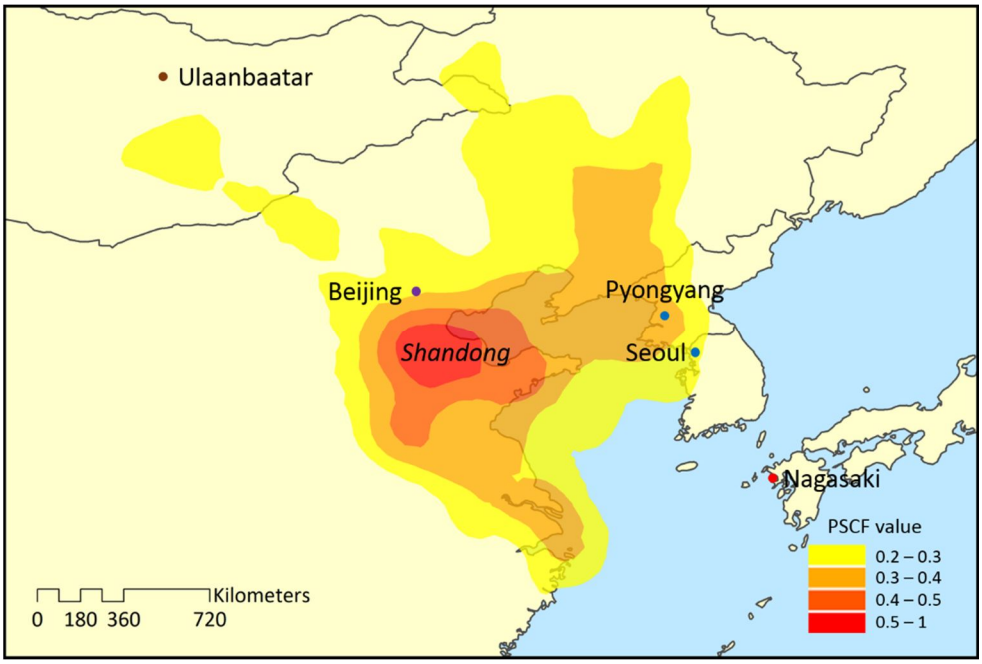

(a) LRT event

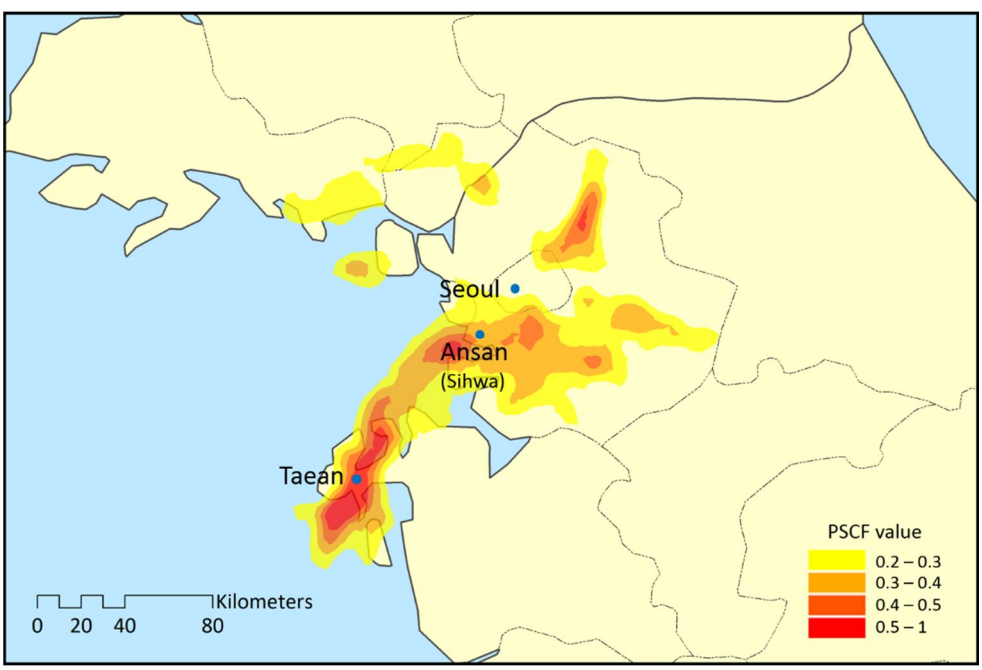

(b) Local event

Fig. 11. PSCF plots for $PM_{2.5}$ in Seoul.

4.3.3. Nagasaki

In the PSCF map for LRT event in Nagasaki (Fig. 12), a couple of areas on the Yellow Sea were indicated as high potential source areas. The SO_2 emissions from coastal areas were originated from oil-fired boilers on heavy vessels and the oxidation of dimethyl sulfide as the product of the digestion of waste sludge in the surface sediments (Gao et al., 1993). The SO_2 emissions from the coastal areas were also caused by numerous international passenger liners (Endresen et al., 2003) between South Korean port cities (Incheon, Gunsan, Busan and Jeju) and Chinese cities (Weihai, Yantai, Qingdao and Shanghai), domestic passenger ships, and fishing boats on the ocean. In addition, the routes between South Korean port cities (Gunsan, Mokpo and Jeju) and Shanghai might represent possible pathways of transport, since Shanghai is one of the largest cities and the most industrialized city in China accommodating 23.9 million people and over 6300 km^2 in 2013.

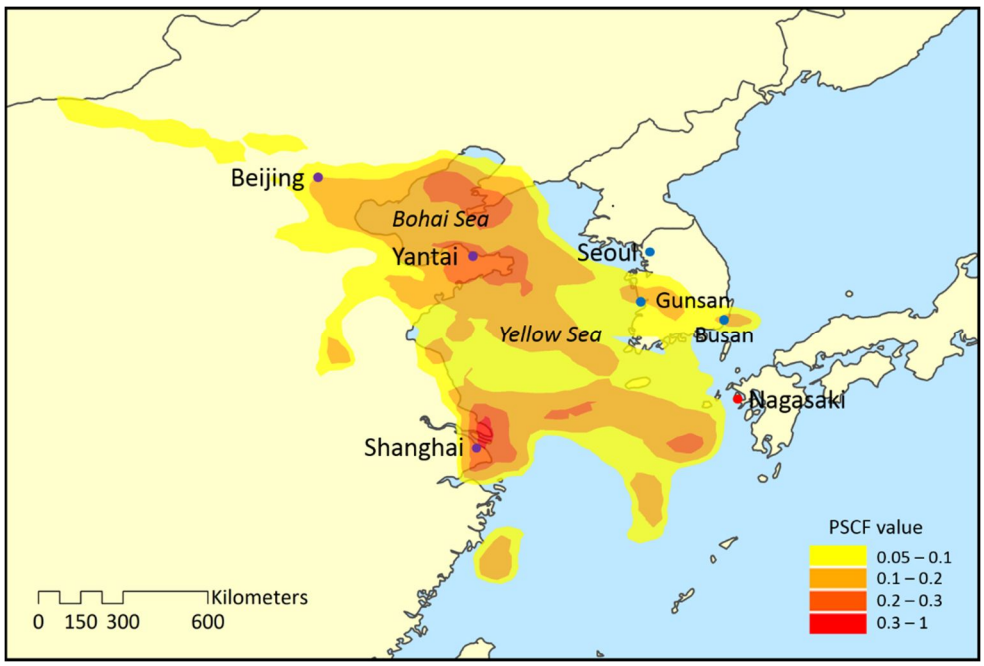

LRT event

Fig. 12. PSCF plots for $PM_{2.5}$ in Nagasaki.

4.4. Time series

Figure 13 to Figure 15 showed the time series of $PM_{2.5}$ concentration in the three cities during sampling period. $PM_{2.5}$ concentration of Beijing (black dot) was referred to the StateAir, U. S. Department of State Air Quality Monitoring Program (http://www.stateair.net/). Red box showed the sections which LRT of high concentration $PM_{2.5}$ were expected, since the concentrations of $PM_{2.5}$ in Seoul and Nagasaki were high in order after the concentrations of $PM_{2.5}$ in Beijing were high, also showed the mixed section of LRT event and Local event. Expected sections that LRT of $PM_{2.5}$ by time series considerably corresponded with LRT event classified by RTA. It was suggested that increasing $PM_{2.5}$ concentrations in Seoul were affected by China, especially in Beijing. Also, this suggested that high concentrations of $PM_{2.5}$ in Nagasaki were caused by the direct inflow of $PM_{2.5}$ from China and South Korea.

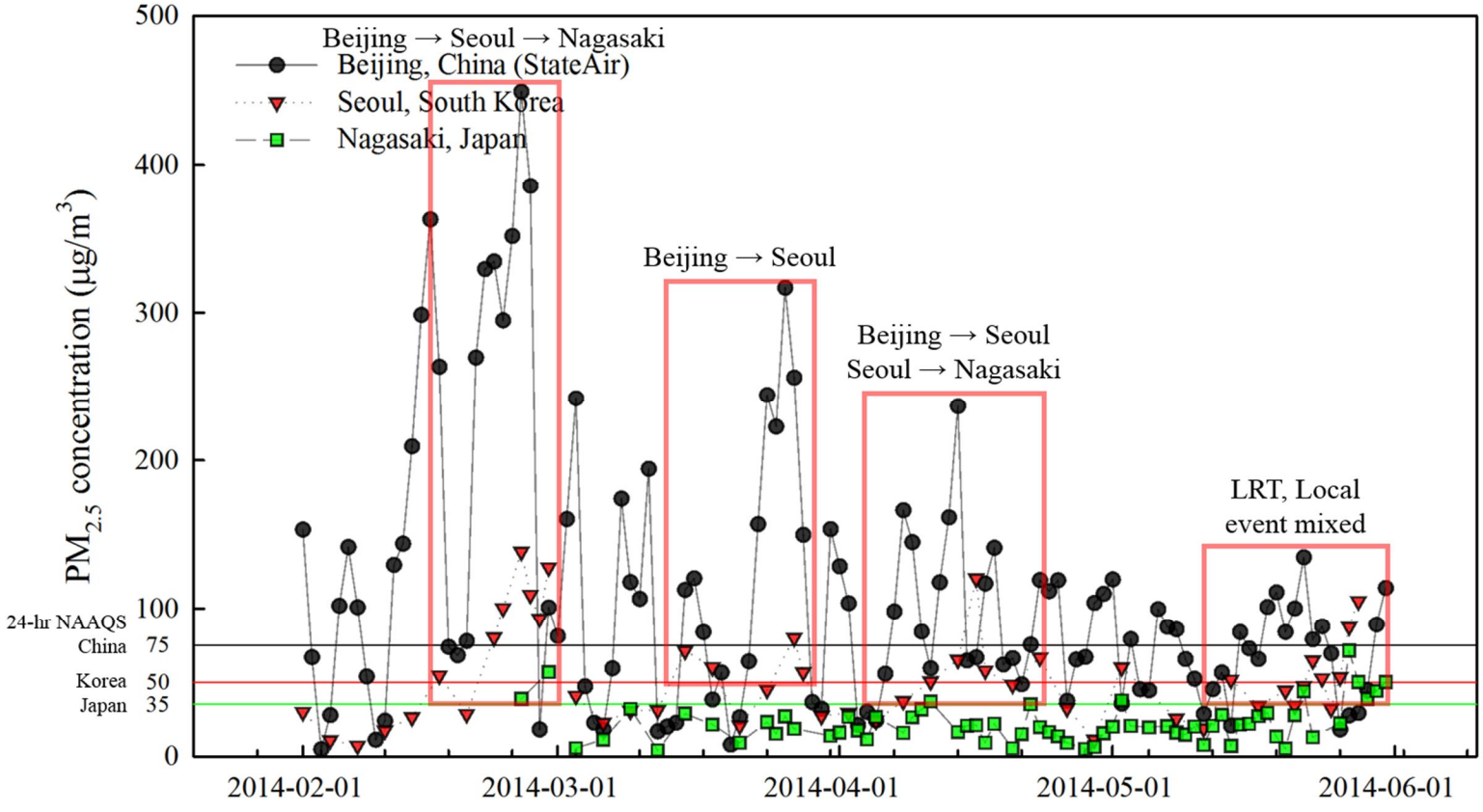

Fig. 13. Time series for $PM_{2.5}$ concentrations in Beijing, Seoul and Nagasaki (2014-02-01~2014-06-01)

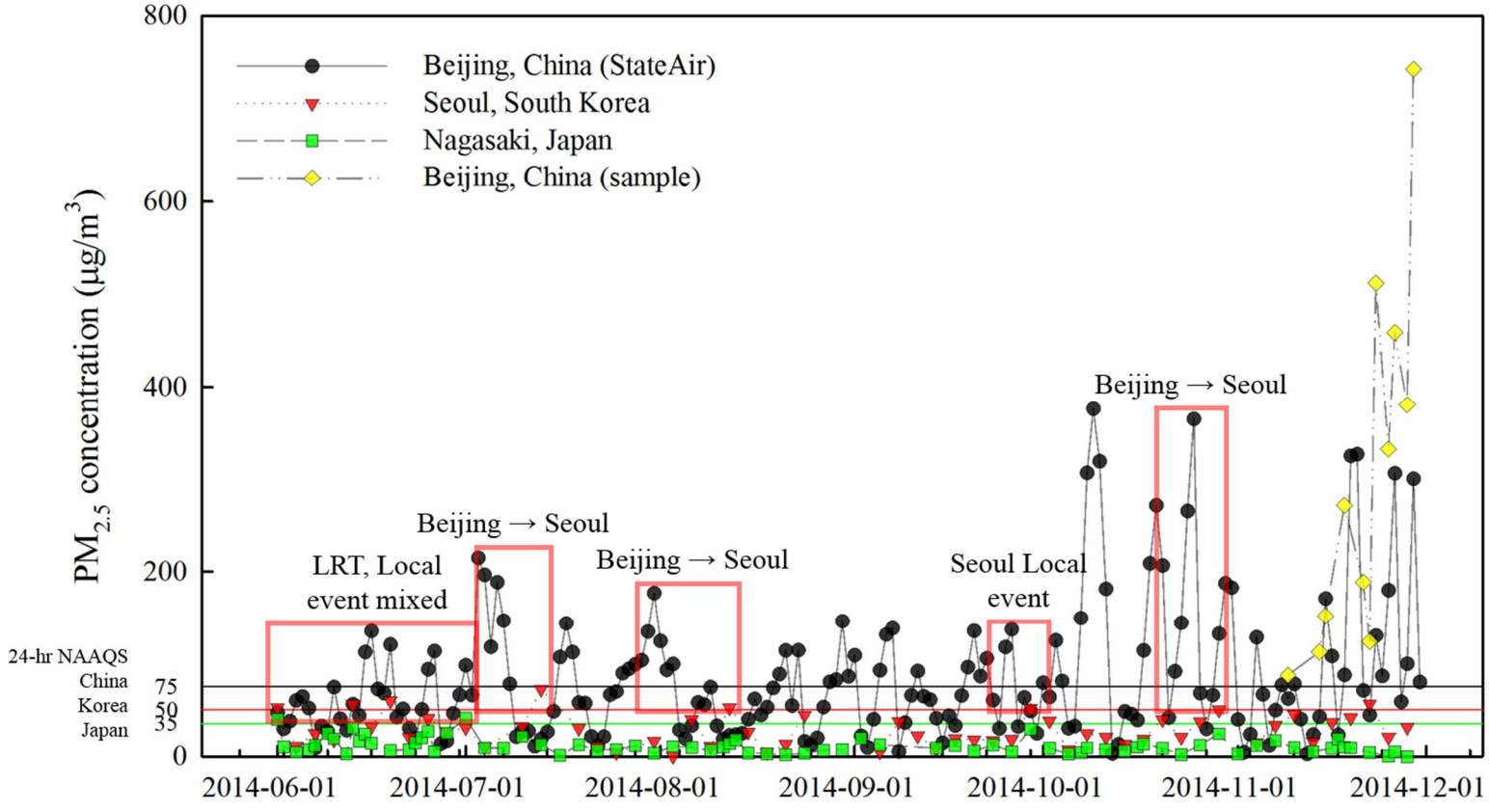

Fig. 14. Time series for $PM_{2.5}$ concentrations in Beijing, Seoul and Nagasaki (2014-06-01~2014-12-01)

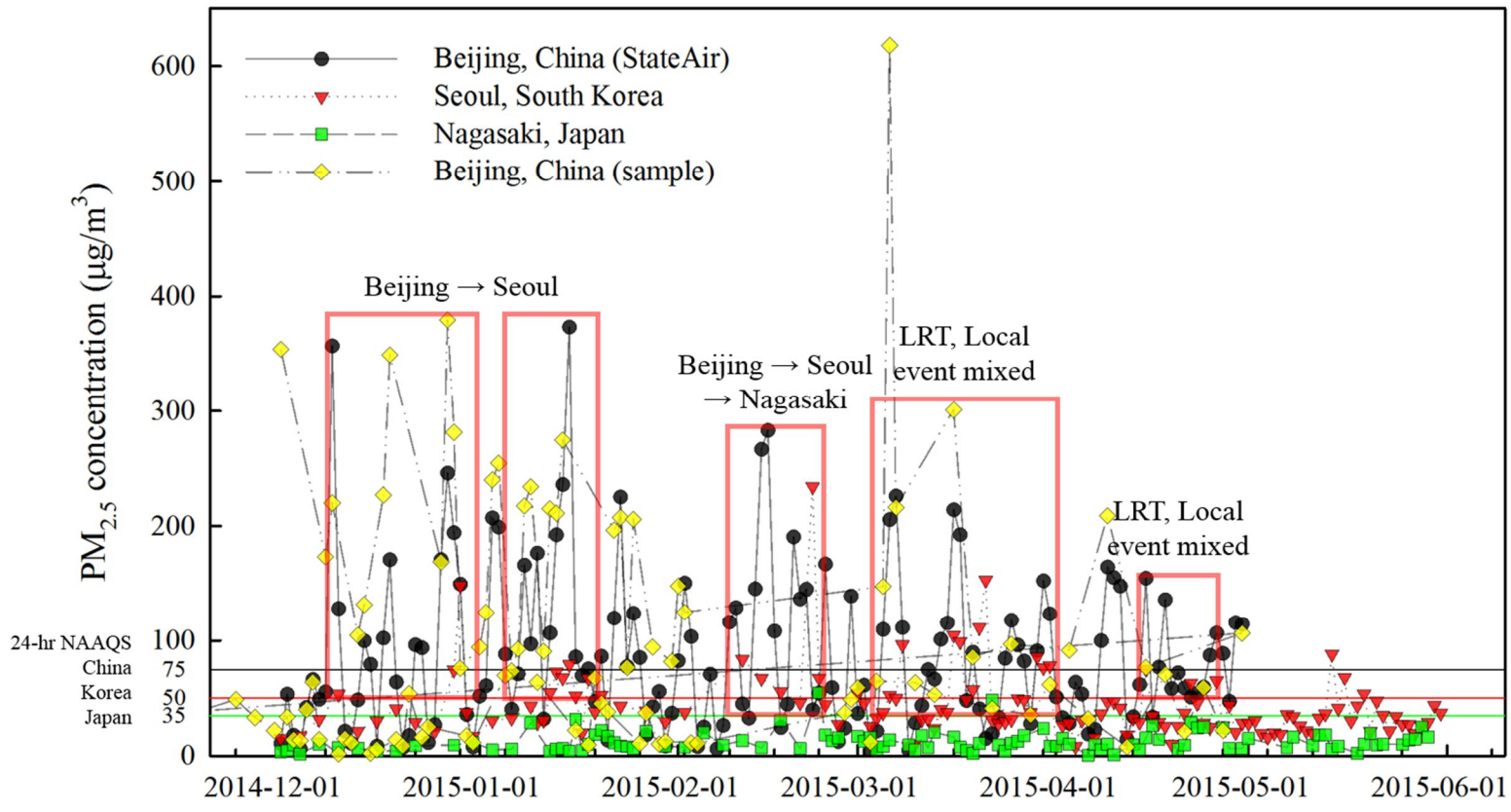

Fig. 15. Time series for $PM_{2.5}$ concentrations in Beijing, Seoul and Nagasaki (2014-12-01~2015-06-01)

5. Conclusions

To identify characteristics of high $PM_{2.5}$, HCEs of $PM_{2.5}$ were classified according to the NAAQS of 24-h $PM_{2.5}$ standard in three countries. And then daily backward trajectories were calculated by RTA and HCEs samples were sorted into LRT events and Local events. HCEs of Beijing were 52 days (out of total 111 sampling days), LRT events were 14 days. In Seoul, HCEs were 92 days (out of total 279 sampling days), LRT events were 64 days. In Nagasaki, HCEs were only 15 days (out of total 245 days), LRT events were 13 days. The $PM_{2.5}$ average concentration of Beijing, Seoul and Nagasaki were found 118, 44 and 18 $\mu g/m^3$ in total, 151, 79 and 48 $\mu g/m^3$ in LRT event and 238, 65, 48 $\mu g/m^3$ in Local event, respectively. It has been suggested that high $PM_{2.5}$ and sulfate concentrations were affected by combustion of fossil fuels and rapid industrialization in China. In Beijing, frequency of Local event was higher than that of LRT event and the effect was more significant when PM2.5 average mass concentration was weighted. On the other hand, in Seoul and Nagasaki, frequencies of LRT event were higher than those of Local event.

The mass ratios of NO_3^- to SO_4^{2-} of Beijing, Seoul and Nagasaki were found 2.13, 1.08 and 1.03 in total, 3.15, 1.06 and 0.86 in LRT event and 2.08, 1.32, 0.14 in Local event with lower ratio indicating the dramatic increase of SO_4^{2-} concentrations, and this was related to stationary sources.

Higher OC/EC values in sampling site demonstrated that SOA was abundant. Good OC–EC correlations were obtained with Pearson correlation coefficient (R) of 0.946, 0.730 and 0.920 for total sampling days, LRT event and Local event in Beijing, respectively. These correlations indicated the presence of common dominant sources for OC and EC.

Different air parcels traveled through different regions and brought different chemical species with the aerosols. In LRT event of Beijing, the trajectories were categorized into 2 sectors for LRT events and 3 sectors for Local events. Air parcels considerably affected by LRT since backward trajectories passed through Russia, Kazakhstan and Mongolia, where the regions that include abundant potassium and crustal elements. In Seoul, the trajectories were categorized into 5 sectors for LRT events and 3 sectors for Local events. The longer the air parcels transported, the higher the starting heights of trajectories and altitudes of air parcels tended to be. Concentrations of sulfur and sulfate were increased when backward trajectory passed through the Yellow sea and industrial area of East China for a long time, relatively. Sulfur was emitted from the combustion of fossil fuel in industrial area of East China passed through sea and the production of aerosol sulfate was enhanced in air that contained a significant amount of seal-salt aerosol. Clusters of Nagasaki were affected by westerlies and were classified by lengths of backward trajectories. For LRT event of Nagasaki, concentrations of crustal elements were significantly higher when air parcels passed through desert of China and Mongolia.

According to LRT event and Local event in three cities, PSCF results showed different possible source areas contributing to the elevated $PM_{2.5}$ concentration. In

Beijing, PSCF results of LRT event, it could be seen that high PSCF values for $PM_{2.5}$ were found along east Kazakhstan. For Local event, the areas near Bohai Bay in southeast Beijing were identified as potential sources. For LRT event of Seoul, it could be seen that high PSCF values for $PM_{2.5}$ were found along Shandong Province. For Local event, it could be seen that high PSCF values were found nearby Seoul, especially Taean an Ansan. Major point sources such as thermoelectric power plants and petrochemical complexes are located in Taean and hundreds of industrial factory are located in Ansan. In the PSCF map for LRT event in Nagasaki, a couple of areas on the Yellow Sea were identified as high possible source areas. Time series of $PM_{2.5}$ concentrations in three cities indicated the possibility of the air parcels movements including high concentrations of $PM_{2.5}$

5. References

Abdalmogith, S.S., Harrison, R.M., 2005. The use of trajectory cluster analysis to examine the long-range transport of secondary inorganic aerosol in the UK. Atmos. Environ. 39, 6686–6695.

Arimoto, R., Duce, R.A., Savoie, D.L., Prospero, J.M., Talbot, R., Cullen, J.D., Tomza, U., Lewis, N.F., Ray, B.J., 1996. Relationships among aerosol constituents from Asia and the North Pacific during PEM-West A. J. Geophys. Res. Atmospheres 1984–2012 101, 2011–2023.

Ashbaugh, L.L., Malm, W.C., Sadeh, W.Z., 1985. A residence time probability analysis of sulfur concentrations at grand Canyon National Park. Atmospheric Environ. 1967 19, 1263–1270.

Birch, M.E., Cary, R.A., 1996. Elemental Carbon-Based Method for Monitoring Occupational Exposures to Particulate Diesel Exhaust. Aerosol Sci. Technol. 25, 221–241.

Borge, R., Lumbreras, J., Vardoulakis, S., Kassomenos, P., Rodríguez, E., 2007. Analysis of long-range transport influences on urban PM10 using two-stage atmospheric trajectory clusters. Atmos. Environ. 41, 4434–4450.

Brunekreef, B., Holgate, S.T., 2002. Air pollution and health. The Lancet 360, 1233–1242.

Cao, J.J., Lee, S.C., Ho, K.F., Zou, S.C., Fung, K., Li, Y., Watson, J.G., Chow, J.C., 2004. Spatial and seasonal variations of atmospheric organic carbon and elemental carbon in Pearl River Delta Region, China. Atmos. Environ. 38, 4447–4456.

Chan, C.K., Yao, X., 2008. Air pollution in mega cities in China. Atmos. Environ. 42, 1–42.

Cheng, S., Yang, L., Zhou, X., Wang, Z., Zhou, Y., Gao, X., Nie, W., Wang, X., Xu, P., Wang, W., 2011. Evaluating PM2.5 ionic components and source apportionment in Jinan, China from 2004 to 2008 using trajectory statistical methods. J. Environ. Monit. 13, 1662.

Chu, S.-H., 2005. Stable estimate of primary OC/EC ratios in the EC tracer method. Atmos. Environ. 39, 1383–1392.

Docherty, K.S., Stone, E.A., Ulbrich, I.M., DeCarlo, P.F., Snyder, D.C., Schauer, J.J., Peltier, R.E., Weber, R.J., Murphy, S.M., Seinfeld, J.H., Grover, B.D., Eatough, D.J., Jimenez, J.L., 2008. Apportionment of Primary and Secondary Organic Aerosols in Southern California during the 2005 Study of Organic Aerosols in Riverside (SOAR-1). Environ. Sci. Technol. 42, 7655–7662.

Dockery, D.W., Pope, C.A., 1994. Acute respiratory effects of particulate air pollution. Annu. Rev. Public Health 15, 107–132.

Draxler, R.R., Rolph, G.D., 2003. HYSPLIT (HYbrid Single-Particle Lagrangian Integrated Trajectory) model access via NOAA ARL READY website (http://www. arl. noaa. gov/ready/hysplit4. html). NOAA Air Resources Laboratory, Silver Spring.

Draxler, R., Stunder, B., Rolph, G., Stein, A., Taylor, A., 2009. HYSPLIT4 user's guide, Ver. 4.9.

Duvall, R.M., Majestic, B.J., Shafer, M.M., Chuang, P.Y., Simoneit, B.R.T., Schauer, J.J., 2008. The water-soluble fraction of carbon, sulfur, and crustal elements in Asian aerosols and Asian soils. Atmos. Environ., Selected Papers from the First International Conference on Atmospheric Chemical Mechanisms 42, 5872–5884.

Endresen, Ø., Sørg\a ard, E., Sundet, J.K., Dalsøren, S.B., Isaksen, I.S., Berglen, T.F., Gravir, G., 2003. Emission from international sea transportation and environmental impact. J. Geophys. Res. Atmospheres 1984–2012 108.

Fuzzi, S., Andreae, M.O., Huebert, B.J., Kulmala, M., Bond, T.C., Boy, M., Doherty, S.J., Guenther, A., Kanakidou, M., Kawamura, K., Kerminen, V.-M., Lohmann, U., Russell, L.M., Pöschl, U., 2006. Critical assessment of the current state of scientific knowledge, terminology, and research needs concerning the role of organic aerosols in the atmosphere, climate, and global change. Atmos Chem Phys 6, 2017–2038.

Gao, N., Cheng, M.-D., Hopke, P.K., 1993. Potential source contribution function analysis and source apportionment of sulfur species measured at Rubidoux, CA during the Southern California Air Quality Study, 1987. Anal. Chim. Acta 277, 369–380.

Geng, H., Park, Y., Hwang, H., Kang, S., Ro, C.-U., 2009. Elevated nitrogen-containing particles observed in Asian dust aerosol samples collected at the marine boundary layer of the Bohai Sea and the Yellow Sea. Atmos Chem Phys 9, 6933–6947.

Hallquist, M., Wenger, J.C., Baltensperger, U., Rudich, Y., Simpson, D., Claeys, M., Dommen, J., Donahue, N.M., George, C., Goldstein, A.H., Hamilton, J.F., Herrmann, H., Hoffmann, T., Iinuma, Y., Jang, M., Jenkin, M.E., Jimenez, J.L., Kiendler-Scharr, A., Maenhaut, W., McFiggans, G., Mentel, T.F., Monod, A., Prévôt, A.S.H., Seinfeld, J.H., Surratt, J.D., Szmigielski, R., Wildt, J., 2009. The formation, properties and impact of secondary organic aerosol: current and emerging issues. Atmos Chem Phys 9, 5155–5236.

Healy, R.M., Sciare, J., Poulain, L., Kamili, K., Merkel, M., Müller, T., Wiedensohler, A., Eckhardt, S., Stohl, A., Sarda-Estève, R., McGillicuddy, E., O'Connor, I.P., Sodeau, J.R., Wenger, J.C., 2012. Sources and mixing state of size-resolved elemental carbon particles in a European megacity: Paris. Atmos Chem Phys 12, 1681–1700.

Heo, J.-B., Hopke, P.K., Yi, S.-M., 2009. Source apportionment of PM2.5 in Seoul, Korea. Atmos Chem Phys 9, 4957–4971.

He, Z., Kim, Y.J., Ogunjobi, K.O., Hong, C.S., 2003. Characteristics of PM2.5 species and long-range transport of air masses at Taean background station, South Korea. Atmos. Environ. 37, 219–230.

Hopke, P.K., 2003. Recent developments in receptor modeling. J. Chemom. 17, 255–265.

Hsu, Y.-K., Holsen, T.M., Hopke, P.K., 2003. Comparison of hybrid receptor models to locate PCB sources in Chicago. Atmos. Environ. 37, 545–562.

Hwang, I., Hopke, P.K., 2007. Estimation of source apportionment and potential source locations of PM2.5 at a west coastal IMPROVE site. Atmos. Environ. 41, 506–518.

III, C.A.P., Dockery, D.W., 2006. Health Effects of Fine Particulate Air Pollution: Lines that Connect. J. Air Waste Manag. Assoc. 56, 709–742.

James, D.E., 1982. A combined O, Sr, Nd, and Pb isotopic and trace element study of crustal contamination in central Andean lavas, I. Local geochemical variations. Earth Planet. Sci. Lett. 57, 47–62.

Jeong, U., Kim, J., Lee, H., Jung, J., Kim, Y.J., Song, C.H., Koo, J.-H., 2011. Estimation of the contributions of long range transported aerosol in East Asia to carbonaceous aerosol and PM concentrations in Seoul, Korea using highly time resolved measurements: a PSCF model approach. J. Environ. Monit. 13, 1905–1918.

Jorba, O., Pérez, C., Rocadenbosch, F., Baldasano, J., 2004. Cluster Analysis of 4-Day Back Trajectories Arriving in the Barcelona Area, Spain, from 1997 to 2002. J. Appl. Meteorol. 43, 887–901.

Junquera, V., Russell, M.M., Vizuete, W., Kimura, Y., Allen, D., 2005. Wildfires in eastern Texas in August and September 2000: Emissions, aircraft measurements, and impact on photochemistry. Atmos. Environ. 39, 4983–4996. doi:10.1016/j.atmosenv.2005.05.004

Kalnay, E., Kanamitsu, M., Kistler, R., Collins, W., Deaven, D., Gandin, L., Iredell, M., Saha, S., White, G., Woollen, J., Zhu, Y., Leetmaa, A., Reynolds, R., Chelliah, M., Ebisuzaki, W., Higgins, W., Janowiak, J., Mo, K.C., Ropelewski, C., Wang, J., Jenne, R., Joseph, D., 1996. The NCEP/NCAR 40-Year Reanalysis Project. Bull. Am. Meteorol. Soc. 77, 437–471.

Kang, C.-M., Lee, H.S., Kang, B.-W., Lee, S.-K., Sunwoo, Y., 2004. Chemical characteristics of acidic gas pollutants and PM2.5 species during hazy episodes in Seoul, South Korea. Atmos. Environ. 38, 4749–4760.

Kim, H.-S., Huh, J.-B., Hopke, P.K., Holsen, T.M., Yi, S.-M., 2007. Characteristics of the major chemical constituents of PM2.5 and smog events in Seoul, Korea in 2003 and 2004. Atmos. Environ. 41, 6762–6770.

Kong, S., Han, B., Bai, Z., Chen, L., Shi, J., Xu, Z., 2010a. Receptor modeling of PM2.5, PM10 and TSP in different seasons and long-range transport analysis at a coastal site of Tianjin, China. Sci. Total Environ. 408, 4681–4694.

Lee, P.K.H., Brook, J.R., Dabek-Zlotorzynska, E., Mabury, S.A., 2003. Identification of the Major Sources Contributing to PM2.5 Observed in Toronto. Environ. Sci. Technol. 37, 4831–4840.

Li, P., Xin, J., Bai, X., Wang, Y., Wang, S., Liu, S., Feng, X., 2013. Observational Studies and a Statistical Early Warning of Surface Ozone Pollution in Tangshan, the Largest Heavy Industry City of North China. Int. J. Environ. Res. Public. Health 10, 1048–1061.

Li, S., Xu, T., Sun, P., Zhou, Q., Tan, H., Hui, S., 2008. NOx and SOx emissions of a high sulfur self-retention coal during air-staged combustion. Fuel 87, 723–731.

Luo, Z., Rossow, W.B., 2004. Characterizing Tropical Cirrus Life Cycle, Evolution, and Interaction with Upper-Tropospheric Water Vapor Using Lagrangian Trajectory Analysis of Satellite Observations. J. Clim. 17, 4541–4563.

Na, K., Sawant, A.A., Song, C., Cocker III, D.R., 2004. Primary and secondary carbonaceous species in the atmosphere of Western Riverside County, California. Atmos. Environ. 38, 1345–1355.

O'Dowd, C.D., Lowe, J.A., Smith, M.H., 1999. Coupling sea-salt and sulphate interactions and its impact on cloud droplet concentration predictions. Geophys. Res. Lett. 26, 1311–1314.

Park, S.S., Kim, Y.J., Fung, K., 2001. Characteristics of PM2.5 carbonaceous aerosol in the Sihwa industrial area, Korea. Atmos. Environ. 35, 657–665.

Poirot, R.L., Wishinski, P.R., Hopke, P.K., Polissar, A.V., 2001. Comparative Application of Multiple Receptor Methods To Identify Aerosol Sources in Northern Vermont. Environ. Sci. Technol. 35, 4622–4636.

Salvador, P., Artíñano, B., Querol, X., Alastuey, A., 2008. A combined analysis of backward trajectories and aerosol chemistry to characterise long-range transport episodes of particulate matter: The Madrid air basin, a case study. Sci. Total Environ. 390, 495–506.

Saylor, R.D., Edgerton, E.S., Hartsell, B.E., 2006. Linear regression techniques for use in the EC tracer method of secondary organic aerosol estimation. Atmos. Environ. 40, 7546–7556.

Shen, Z., Arimoto, R., Cao, J., Zhang, R., Li, X., Du, N., Okuda, T., Nakao, S., Tanaka, S., 2008. Seasonal Variations and Evidence for the Effectiveness of Pollution Controls on Water-Soluble Inorganic Species in Total Suspended Particulates and Fine Particulate Matter from Xi'an, China. J. Air Waste Manag. Assoc. 58, 1560–1570.

Simoneit, B.R.T., 2002. Biomass burning — a review of organic tracers for smoke from incomplete combustion. Appl. Geochem. 17, 129–162.

Skinner, B.J., 1979. Earth resources. Proc. Natl. Acad. Sci. 76, 4212–4217.

Stohl, A., 1998. Computation, accuracy and applications of trajectories—A review and bibliography. Atmos. Environ. 32, 947–966.

Turpin, B.J., Saxena, P., Andrews, E., 2000. Measuring and simulating particulate organics in the atmosphere: problems and prospects. Atmos. Environ. 34, 2983–3013.

Uematsu, M., Duce, R.A., Prospero, J.M., Chen, L., Merrill, J.T., McDonald, R.L., 1983. Transport of mineral aerosol from Asia Over the North Pacific Ocean. J. Geophys. Res. Oceans 88, 5343–5352.

Wang, X., Bi, X., Sheng, G., Fu, J., 2006. Chemical Composition and Sources of PM10 and PM2.5 Aerosols in Guangzhou, China. Environ. Monit. Assess. 119, 425–439.

Wang, Y., Zhuang, G., Tang, A., Yuan, H., Sun, Y., Chen, S., Zheng, A., 2005. The ion chemistry and the source of PM2.5 aerosol in Beijing. Atmos. Environ. 39, 3771–3784.

Wang, Y., Zhuang, G., Zhang, X., Huang, K., Xu, C., Tang, A., Chen, J., An, Z., 2006. The ion chemistry, seasonal cycle, and sources of PM2.5 and TSP aerosol in Shanghai. Atmos. Environ. 40, 2935–2952.

Xu, X., Akhtar, U.S., 2010. Identification of potential regional sources of atmospheric total gaseous mercury in Windsor, Ontario, Canada using hybrid receptor modeling. Atmospheric Chem. Phys. 10, 7073–7083.

Yao, X., Chan, C.K., Fang, M., Cadle, S., Chan, T., Mulawa, P., He, K., Ye, B., 2002. The water-soluble ionic composition of PM2.5 in Shanghai and Beijing, China. Atmos. Environ. 36, 4223–4234.

Zeng, Y., Hopke, P.K., 1989. A study of the sources of acid precipitation in Ontario, Canada. Atmospheric Environ. 1967 23, 1499–1509.

Zhang, Q., Worsnop, D.R., Canagaratna, M.R., Jimenez, J.L., 2005. Hydrocarbon-like and oxygenated organic aerosols in Pittsburgh: insights into sources and processes of organic aerosols. Atmos Chem Phys 5, 3289–3311.

Zheng, M., Salmon, L.G., Schauer, J.J., Zeng, L., Kiang, C.S., Zhang, Y., Cass, G.R., 2005. Seasonal trends in PM2.5 source contributions in Beijing, China. Atmos. Environ. 39, 3967–3976.

국문초록

베이징, 서울, 나가사키에서 측정한 $PM_{2.5}$의 장거리 이동 및 특성 파악

정승표

서울대학교 보건대학원

환경보건학과 대기환경전공

2013년부터 2015년까지 세 도시(베이징, 서울, 나가사키)에서 대기 중 초미세먼지($PM_{2.5}$)를 채취하였다(베이징: 2014년 11월−2014년 4월, 서울: 2013년 9월−2015년 5월, 나가사키: 2014년 2월−2015년 5월). $PM_{2.5}$의 화학적 구성 성분으로 17가지 미량 원소, 3가지 수용성 이온, 유기 탄소, 원소 탄소를 분석하였다. 중국, 한국, 일본의 대기환경기준을 통해, $PM_{2.5}$의 고농도 사례를 구분하였고 구분한 고농도 사례에 체류 시간 분석을 실시하여 장거리 이동과 국지적 영향으로 구분하였다. 장거리 이동과 국지적 영향의 특성을 파악하기 위하여, NO_3^-/SO_4^{2-}와 OC/EC 질량 농도 비의 특성을 파악하였다. 군집 분석과 potential source

contribution function (PSCF)는 체류 시간 분석 결과와 비교하여 $PM_{2.5}$ 고농도 사례 발생의 특성과 잠재적 오염원을 파악하고자 하였다.

베이징의 $PM_{2.5}$ 고농도 사례는 전체 111일 중 52일이고 장거리 이동에 의해 영향을 받은 날이 14일이었다. 서울은 전체 279일 중 $PM_{2.5}$ 고농도 사례가 92일, 그 중 장거리 이동에 의해 영향을 받은 날이 64일이고 나가사키는 전체 245일 중 $PM_{2.5}$ 고농도 사례가 불과 15일, 그 중 장거리 이동에 의해 영향을 받은 날이 13일이었다. 베이징, 서울, 나가사키의 $PM_{2.5}$ 평균 농도는 전체: 118, 44, 18 $\mu g/m^3$, 장거리 이동: 151, 79, 48 $\mu g/m^3$, 국지적 영향: 238, 65, 48 $\mu g/m^3$ 이었다. $PM_{2.5}$와 SO_4^{2-}의 질량 농도가 중국의 국지적 영향과 한국의 장거리 이동일 경우 높았는데, 이는 중국 내 화석 연료 연소 및 공업화의 영향으로 판단되었다.

군집 분석 결과를 통해, 공기의 역궤적이 중국의 해안지대와 바다를 거쳐 시료 채취 지역으로 도착할 때, SO_4^{2-}의 농도가 통계적으로 유의하게 증가하는 것으로 나타났다. PSCF 결과는 세 도시에 대해, 장거리 이동과 국지적 영향의 오염원 가능 지역이 매우 다르다는 것을 가리켰다. 베이징, 서울, 나가사키의 $PM_{2.5}$ 농도를 시계열 자료로 나타냈고 이는 고농도 $PM_{2.5}$의 세 도시간 이동 가능성이 매우 높다는 것을 의미했다.

주요어: $PM_{2.5}$, 고농도 사례, 장거리 이동 사례, 국지적 영향 사례, 체류 시간 분석, 군집 분석, Potential Source Contribution Function (PSCF)

학번: 2014-23362